POLITECNICO DI TORINO
Master Degree course in Communications and Computer Networks Engineering

Master Degree Thesis

Bandwidth Enhancement of Wavelength Selective Switches to Improve Transmission Performance of Subcarrier-Multiplexed Optical Links

Supervisors
Dr. Dario Pilori
Prof. Roberto Gaudino
Dr. Ann Margareth Rosa Brusin

Candidate
Piernunzio Natuzzi
matricola : 292426

Academic Year 2023-2024

To everyone who believed in me

Acknowledgements

I would like to express my deepest gratitude to my thesis advisors, Dr. Dario Pilori, Prof. Roberto Gaudino and Dr. Ann Margareth Rosa Brusin, for their unvaluable guidance, support and expertise throughout this research. Thank you for your patience and your insightful feedbacks.

Abstract

The analysis presented in this thesis revolves around optical network where signals are routed from the source to the destination using devices known as Reconfigurable Optical Add-Drop Multiplexers (ROADMs). These devices act as both multiplexers and demultiplexers, capable of selecting specific wavelengths and route it to a local RX (Drop) or to choose new traffic to route from a TX (Add) eliminating the need for conversion to and from electrical domain. The core component of the ROADM is the Wavelength Selective Switches (WSS), which acts as filters, ultimately affecting signal quality at the edges of the Frequency Bandwidth.
Furthermore, as optical networks become bigger and bigger, a large number of ROADMs could be required to route the signal properly. As a result, the impact of WSS filtering becomes more significant as the number of cascaded ROADMs, and therefore the number of WSS, increases. Indeed, the main goal of this thesis is to reduce its impact, following different strategies. Firstly the transmitted signal has been divided into subcarriers, each with the same Spectral Bandwidth. The use of multi-sub-carrier systems (MSCs) offers the advantage of assigning different modulation formats to each sub-carrier independently using the Frequency Domain Hybrid Modulation Formats (FDHMF) allowing traffic's heterogeneity and the usage of optimization strategies, such as bit and/or power loading, to enhance system performance. Finally, these techniques have been combined jointly to the use of modern WSS relying on a revised transfer function.
This allows for the introduction of a new technique called "Bandwidth Enhancement", which aims to better exploit Bandwidth Edges to minimize the filtering effect.
In this work, standard Single-Carrier transmission is compared to MSC solution for a system operating at 800 Gbps. Specifically, two modulation format approaches are examined: Uniform Quadrature Amplitude Modulation (QAM) Constellation and Probabilistic Constellation Shaping (PCS). With Uniform QAM Constellation, all symbols are equally probable. In contrast, PCS assigns different probabilities to the symbols, shaping the initial $2^M - QAM$ (where M is an integer number) constellation enabling rate flexibility and increased spectral efficiency.
As final outcome, the application of these techniques has shown that MSC systems generally outperform Single-Carrier one when multiple WSS are present.

Contents

List of Figures

List of Tables

Chapter 1

Introduction

In this introductory chapter some useful concepts will be introduced to better understand the whole thesis. As a main reference, it has been considered [1].

1.1 Optical Networks

Telecommunication systems have revolutionized the way we connect, making it possible to share huge amounts of information over great distances. The simplest topology of a Communication System is the Point-to-Point scheme and it's composed of a Transmitter (TX), a Receiver (RX) and a channel (i.e. Optical Fiber for optical communication systems) connecting the two as depicted in Fig. 1.1. Nowadays, Optical Networks can be considered the backbone of modern telecommunication systems, supporting everything from high-speed internet and telecommunications to cloud computing and streaming media. The term "network" is formally defined as a set of *nodes* connected to each other through *links*. Specifically, in optical networks, nodes perform data processing, forwarding, and routing operations, whereas links serve as communication media along which data are shared. A schematic representation of an optical network is shown in Fig.1.2.

Moreover, depending on the placement and connections of nodes in the network, different types of network topologies can be defined, such as mesh, ring, tree, star, and so on as depicted in Fig.1.3 . Optical networks are largely used to share data traffic worldwide, relying on the use of optical fiber over which light waves are transmitted, representing data in binary form or, more precisely, symbols that carry information. The optical signals are usually generated by Lasers or LEDs, depending on the application field, with either direct or external modulator employed to convert binary data in electric form into optical signal, modeling it according to the applied voltage. For instance, in short reach optical links, LEDs can be used, whereas in long-haul or ultra long-haul application, Lasers with an external modulator are necessary. The generated signal propagates through the optical fiber, allowing for incredibly fast and efficient transmission with minimal signal loss. Optical networks can be classified according to their links' length into:

1. *Access Network:* used to connect the end user to the nearest central office, only a few kilometers long.

2. *Metropolitan Network:* interconnects nearby central offices, typically up to 100 Km.

3. *Long Haul Network:* allows countries and continents' interconnection even through submarine networks, with a length of thousands of kilometers.

Figure 1.1: Schematic representation of a Point to Point Communication System

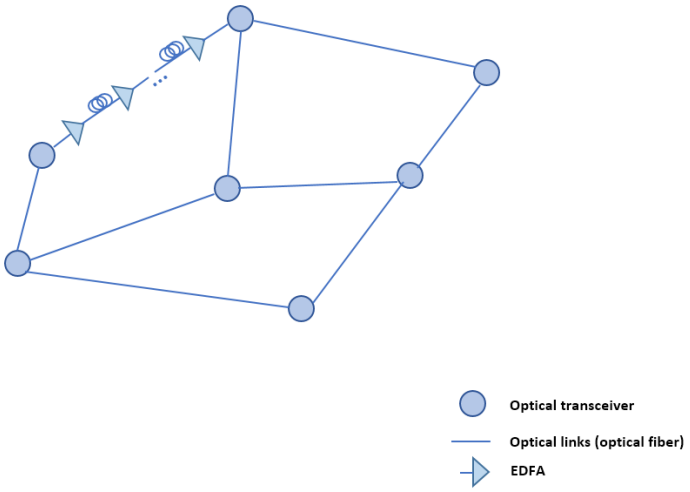

Figure 1.2: Schematic representation of an optical network. EDFA: Erbium Doped Fiber Amplifier; transceiver: TX+RX

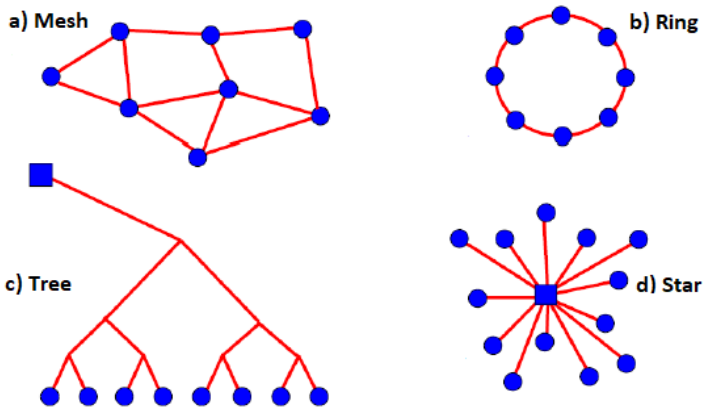

Figure 1.3: Examples of the mostly used network topologies in optical networks

1.2 Optical Fiber Links

1.2.1 Optical Fiber Structure

The links in optical communication systems are made of optical fiber. This transmission media is usually made of purified Silica glass (SiO_2) and its structure can be divided into three concentric sections as shown in Fig. 1.4.

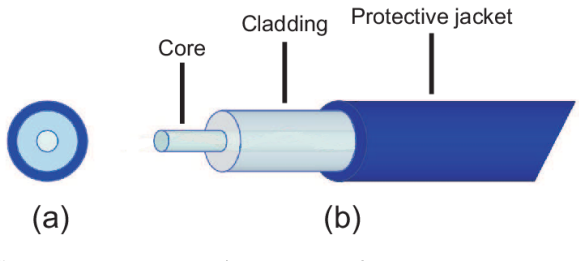

Figure 1.4: Schematic diagram of an optical fiber illustrating:(a) cross section (b) side on view [2]

- The *core* is the inner part.
- The *cladding* is the layer that surrounds the core. Its refractive index *(n_{cl})*, a parameter that defines how a certain material interacts with an electromagnetic field propagating within it, is lower than that of the core *(n_{co})*.
- The outer part is the *coating*. It contains several sub-layers, usually made of plastic,that aim at protecting the fiber from mechanical shocks and damages.

Furthermore, optical fibers can be classified, according to the number of propagated modes, into Single Mode Fibers (SMF) and Multi Mode Fibers (MMF). The first one has a core diameter typically around 10 μm wide while for the latter this dimension can range between 50 μm and 100 μm. In SMF only one mode is allowed, producing low dispersion and small attenuation, making it the best choice for Long-Haul communications.
When a properly focused and aligned laser beam hits the end face of a fiber, its power mostly propagates in the fiber core. However, a non negligible part of the power, may propagate in the cladding as cladding modes. Depending on the properties of the surrounding coating, cladding modes may either propagate over long distances or may be strongly attenuated by leakage into the coating. The latter situation is common particularly for SMFs [3].
In optical transmission, the "Dispersion" can be either Chromatic or Modal. With this thesis being centered around SMF, only Chromatic Dispersion (CD) will be taken into consideration. As a matter of fact, CD is the most important linear distortion effect in optical transmission. It is caused by the variation of group velocity (propagation speed) with optical frequency. The group velocity is defined as the velocity at which a packet of wavelengths travels along the fiber. CD's relevance increases with bit rate and/or distance, although the newest coherent receivers are able to compensate for it using the Digital Signal Processing (DSP), thus, shifting dispersion management to the electrical domain. This makes the long-haul communication systems more robust to signal distortion like CD and simplifies the design and deployment of optical networks.
The term *"Attenuation"* refers to the power reduction of the input signal transmitted along the fiber. It occurs in both Multi-Mode and Single Mode transmission but is exceptionally low for fibers compared to all other guided transmission media. Indeed, in the typical frequency range used for long-haul fiber-optic communications (the so-called C-band, which goes from 191 to 196 THz / 1530 nm to 1570 nm), the attenuation is of about 0.2 dB/km (Fig. 1.5). Furthermore, when long distances are involved in optical communication systems, the attenuation, even with a low value, could represent a problem for the signal propagation due to its proportional increment with the covered distance. An intuitive approach to counteract attenuation could rely on increasing the power of the optical signals launched into the fiber. However, excessively increasing power amplifies nonlinear fiber effects like the Kerr effect, which causes the variation in the glass refractive index as a function of the input power ultimately degrading the system performance. Instead, in long-haul optical systems, *Optical Amplifiers* (Opt.Amp.) are periodically placed along the transmission link.

1.2.2 Optical Amplifiers

Optical Amplifiers are devices used in fiber optic communication systems to amplify optical signals directly, without converting them to and from electrical domain, relying on a physical phenomenon called *"Stimulated Emission"*. These devices play a crucial role in long-haul data transmission, as they boost weakened optical signals over extended fiber lengths, making for efficient and high-capacity networks. The most common optical

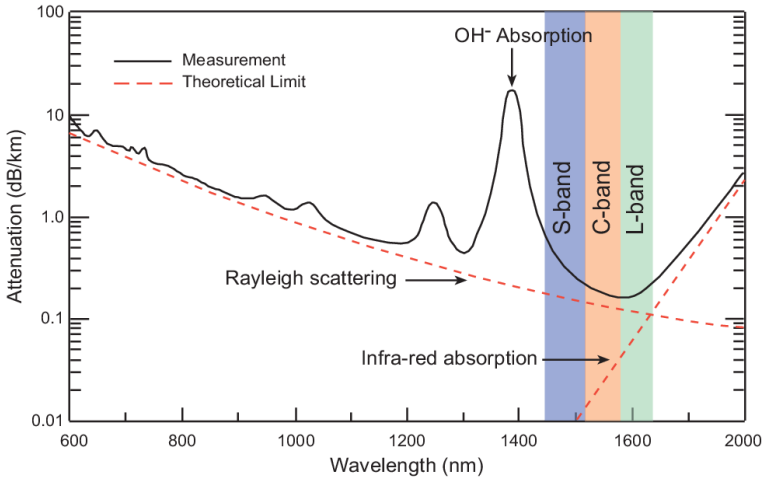

Figure 1.5: Fiber Attenuation vs. Wavelength [2]

amplifiers used in optical communication are:

- *Erbium Doped Fiber Amplifier(EDFA)*: the amplification is performed by injecting a pump laser at a wavelength of either 980 nm or 1480 nm in a piece of fiber whose core is doped with Erbium ions (Er^{3+}).The pumped laser energizes these ions, causing them to switch from a low-energy state to an excited, higher-energy state. When the Erbium ions interact with the incoming optical signal, they partially release their energy as additional photons with the same wavelength, phase and direction of the signal's, effectively boosting it. After this process they return to the initial energy state. A schematic representation of this process is shown in Fig.1.6(a) while in Fig.1.6(b) the EDFA architecture is illustrated. This type of amplifiers works only in L-Band and C-Band, performing very well in the latter where also the fiber attenuation reaches its minimum. Indeed, due to this matching, they are largely used in Long-Haul communications systems.

- *Semiconductor Optical Amplifier(SOA)*: the working principle is similar to the EDFAs but, unlike the previous case, the required energy to induce the stimulated emission derives from the current injected in a P-N junction. Furthermore, this kind of amplifiers is typically used in metro and access networks, thus, for short reach applications as an alternative to EDFAs.

- *Raman Amplifier*: it exploits stimulated Raman scattering in the transmission in order to have a distributed amplification. [4]

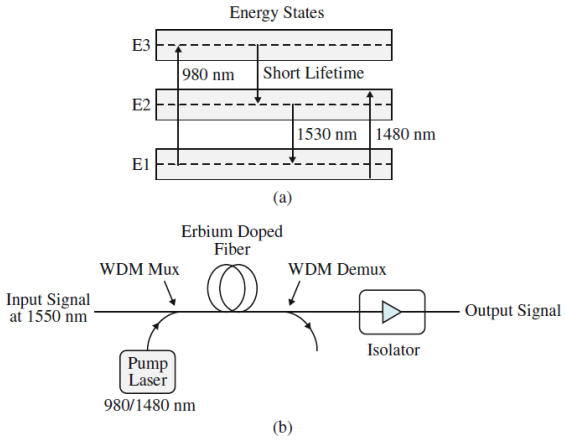

Figure 1.6: (a) amplification process in EDFA, (b) EDFA architecture [5].

Moreover, according to the demanded target distance, it may be necessary to use several Opt. Amp. along the links, to regenerate the weakened optical signals periodically, spaced by a length called span. Thus, a further classification of the optical systems can be done:

- single-span, non amplified systems;
- single-span, optically amplified systems;
- multi-span, optical amplified systems;

A schematic representation of this classification is shown in Figg.1.7,1.8,1.9

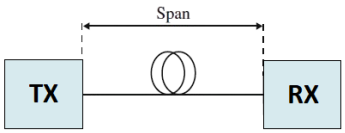

Figure 1.7: Single-span non optically amplified system

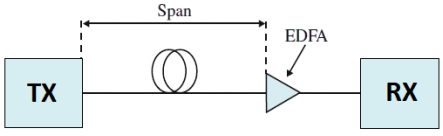

Figure 1.8: Single-span optically amplified system

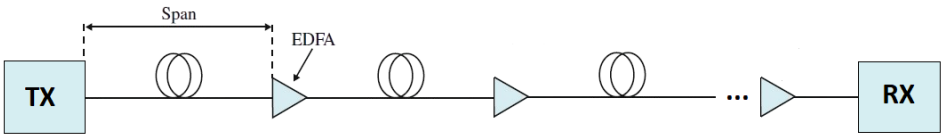

Figure 1.9: Multi-span optically amplified system

1.3 Optical Transceiver [6] [7]

An *Optical Transceiver* is a device that integrates both transmitter and receiver functionalities, enabling the bidirectional conversion of electrical and optical signals. Indeed its main building blocks are: the optical transmitter (Tx) and the optical receiver (Rx). A pictorial representation is shown in Fig.1.10.

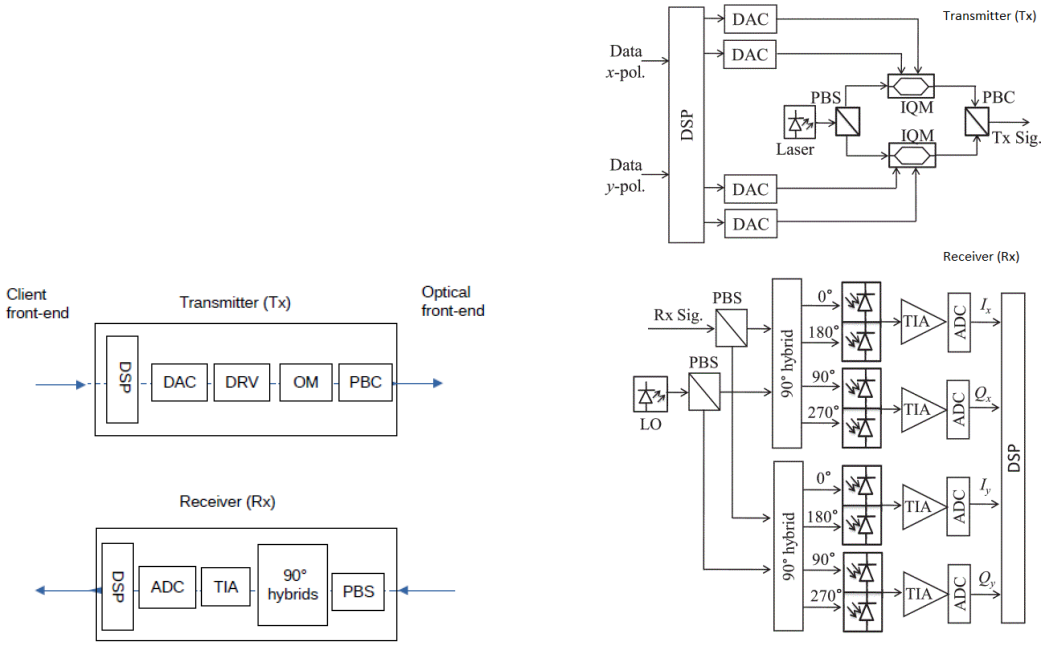

(a) (b)

Figure 1.10: DSP-enabled optical transceiver block diagram (a) [7]; detailed configuration of a DSP-enabled optical transceiver (b) [6].

1.3.1 Optical Transmitter

In an optical transmitter, several operations are done to transform streams of bits received as input into optical signals, to be transmitted over fiber, with high spectral efficiency in order to fully exploit the available bandwidth. In Fig.1.10(a), these operations are depicted in a block diagram. Furthermore, in today's optical transmitter used for long haul applications, a first DSP optimization stage is performed. This may include encoding, pre-compensation of linear and nonlinear transmission impairments and pulse shaping filtering. Then, the signal is converted into analog signals using four digital-to-analog converters (DACs) and then modulated by modulator drivers (DRVs) to preserve signal quality. Next, the Optical Modulator (OM) generates the signal with in-phase and quadrature components, which are subsequently combined by a Polarization Beam Combiner (PBC) for transmission in the optical domain.

Optical Modulator

Two main different types of optical modulators can be identified. The first one is the Intensity Modulator (IM). This device encodes digital information by varying optical power instantaneously. Because of this, the only modulation format generated is M - Pulse Amplitude Modulation (M-PAM), with M=2^k being the constellation cardinality where "k" is the number of bits per symbol; some examples of common M-PAM modulations are illustrated in Fig. 1.11. Moreover, the most commonly used optical modulator in nowadays communication systems is the PM-IQ (Polarization Multiplexing In-phase/Quadrature) modulator. As a matter of fact, it is an essential component for high-speed data transmission due to its ability to modulate both amplitude and phase, enabling complex modulation formats like Quadrature Amplitude Modulation (QAM) which are used in this work. A pictorial schematic representation of QAM constellation is shown in Fig. 1.12 while a block diagram of this modulator in Fig. 1.13.

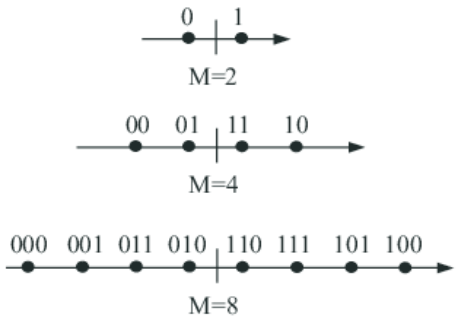

Figure 1.11: M-PAM constellations [8]

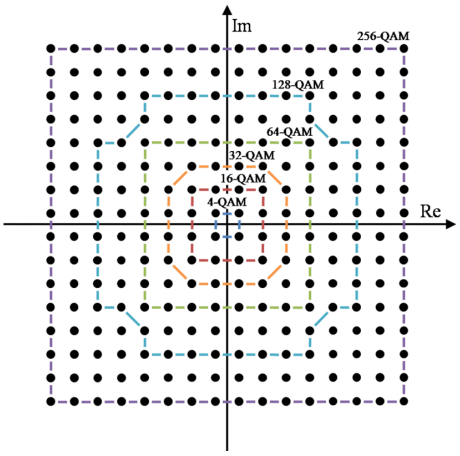

Figure 1.12: QAM constellation diagram [9]

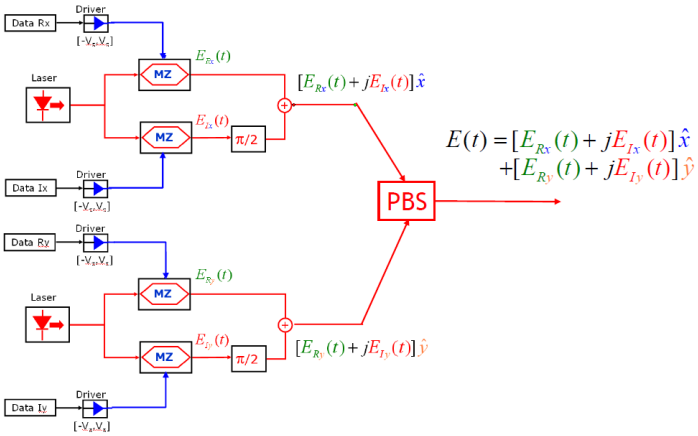

Figure 1.13: PM-I/Q Modulator scheme. PBS: Polarizing Beam Splitter; MZ: Mach-Zehnder modulator [10].

1.3.2 Optical Receiver

Optical Receivers are devices used to retrieve information from incoming signals. They can be firstly classified by considering the method used to convert optical power into electric current. This process of conversion is called *Detection* and can be further classified into Direct Detection (DD) and Coherent Detection (CohD). DD receivers, on the one hand, are based on the first cited method and are simpler and more cost-effective with respect to the coherent counterpart. On the other hand, they can only detect the intensity of the incoming optical signal, converting it, through a single photodiode, directly into an electrical signal without recovering the phase or polarization information.

Thus, DD receivers are able to detect only IM modulation formats like M-PAM. Indeed, this kind of receiver is typically used jointly with the IM at the transmitter, defining the so called IM-DD systems, frequently used in data centers to connect servers and switches and in Passive Optical Networks (PONs) for local access, such as Fiber To The Home (FTTH). Furthermore, in the mid-2000s, to better exploit the available bandwidth resources, the optical community moved fast to develop technologies for spectral efficient transmission [5]. To reach this goal, the correct detection of more complex modulation formats became mandatory. To face this need Coherent Receivers have been introduced, which are able to handle high data rates and complex modulation formats. These receivers are able to detect the information from both the phase and polarization of the signal,thus, exploiting all four degrees of freedom available in the optical fiber. As a result, the electric field propagating in the fiber can be expressed as shown in Eq.1.1.

$$E(t) = [E_{Rx}(t) + jE_{Ix}(t)]\hat{x} + [E_{Ry}(t) + jE_{Iy}(t)]\hat{y} \tag{1.1}$$

In the previous equation, E_{Rx} and E_{Ix} are respectively the Real and the Imaginary components of the x-polarization, while E_{Ry} and E_{Iy} are, simmetrically, the Real and the Imaginary components of the y-polarization. $\hat{x}$ and $\hat{y}$ are unitary vectors along the x and y axes, representing the directions of the orthogonal electric field components. Moreover, the expression 1.1 is described according to the *Jones formalism*, a mathematical model commonly used to describe the polarization state of coherent light by representing the electric field as a combination of two orthogonal components in the complex domain. Furthermore, coherent receivers, thanks to the introduced technologies enhancement compared to the DD RXs, can be defined as a cornerstone of modern optical communication. Their reliance on DSP to compensate linear impairments and Polarization-Sensitive detection, allows them to overcome the challenges of long haul transmission, making this technology fundamental for today's high-capacity networks. A schematic representation is shown in Fig. 1.14, in which the "special optical device" is a 90° Hybrid that allows to extract phase, amplitude and polarization information of the incoming signal by performing interferences between the received field E_{ph} and an external Local Oscillator (LO) signal E_{LO}. Indeed, as it can be noticed from this figure, to obtain all four components of the E_{ph}, the E_{LO} signal must be aligned, both in frequency and in phase, with each component to successful detect it.

1.3.3 Digital Signal Processing (DSP) [11] [12]

DSP plays a critical role in high speed long haul communication systems due to several reasons. Firstly, at the TX it performs operations such as encoding, pre-compensation of linear and nonlinear transmission impairments and pulse shaping filtering, helping in increasing Spectral Efficiency (SE) of the transmitted signals, allowing more data to be transmitted within a limited bandwidth. Consequently, it is essential for the Coherent Receiver to correctly extract the four orthogonal components of the transmitted signal, aligning them with respect to the reference axes, performing phase and clock recovery. Furthermore, it is also used to compensate for signal distortions caused by

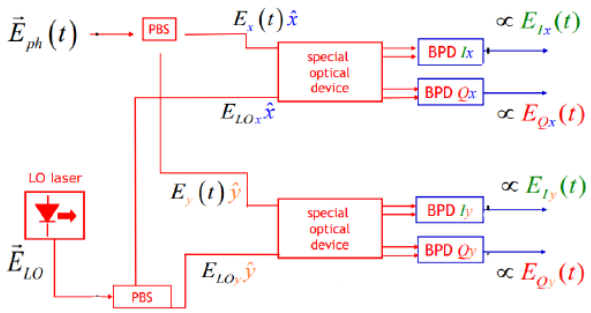

Figure 1.14: Schematic illustration of Coherent RX. BPD: Balanced Photo Detector; special optical device: 90° Hybrid; [10].

impairments like Chromatic Dispersion (CD) and Polarization Mode Dispersion (PMD) and to mitigate non linearity effects such as fiber non linearity, typically present in Dense Wavelength Division Multiplexing systems (DWDM) particularly in high power applications. Additionally, it brings the network to be more flexible and adaptive since it can dynamically adjust modulation formats and other parameters in response to network conditions, optimizing for either higher capacity or greater reach depending on the demand. Furthermore, DSP also includes Error Correction algorithms like FEC, enabling more reliable systems over huge distances without needing excessive retransmission. DSP has been implemented in this thesis by exploiting the *OptDSP* library in MATLAB and a block diagram of its operational chain is shown in Fig. 1.15.

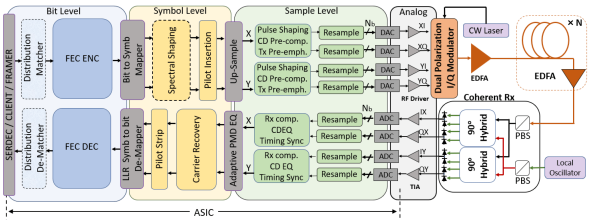

Figure 1.15: Block diagram of a Coherent DSP modem. FEC ENC: Forward Error Correction Encoder; CW laser: Continuous-Wave laser; CD EQ: Chromatic Dispersion equalizer; FEC DEC: Forward Error Correction Decoder [11].

1.4 Digital Subcarrier Multiplexing

A central topic of this thesis is Digital Subcarrier Multiplexing. This technique has been introduced to split a high-baud-rate Single Carrier (SC) signal into multiple low-baud-rate subcarriers. Moreover, to use this functionality, it has been required an enhancement

in high-speed Digital-to-Analog Converter (DAC) and by incorporating Digital Signal Processing (DSP) not only at the receiver, where it is essential, but also at the transmitter. For instance, given a total Baud Rate of 24 GBaud, dividing the signal into two subcarriers results in each subcarrier having a baud rate of 12 GBaud; dividing it into four results in 6 GBaud per subcarrier, and so forth. In Fig. 1.16 an example of a frequency channel divided into subcarriers is depicted.

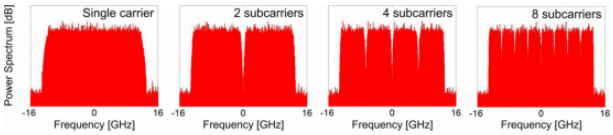

Figure 1.16: Power spectra of the SC signal and MSC signals [13]

Digital Subcarrier Multiplexing is recognized as an effective candidate for mitigating fiber nonlinearity and to reduce the DSP algorithm complexity [14]. Throughout this work, the Multi-Subcarrier (MSC) approach will be consistently compared with its Single Carrier counterpart.Furthermore, the number of subcarriers used will be varied to identify the optimal configuration. Additionally, in this analysis, the MSC approach is applied using techniques for two main constellations types: Uniform QAM Constellation (2^M-QAM, where M is an integer number and denotes the constellation cardinality) and Probabilistic Constellation Shaping (PCS).

1.5 Goal and organization of the thesis

In general, to fully exploit channel resources, they are shared through time, frequency/wavelength, space or code division multiplexing and multiple access techniques. In optical communications the most common used of these techniques is the Wavelength Division Multiplexing (WDM). Indeed, the use of WDM allows the outputs of several transceivers, operating in different wavelengths, to be optically multiplexed using a multiplexer and sent into a single fiber. Then at the receiver side, a multi port filter called WDM demultiplexer is used to separate each WDM channel. In this work a WDM system will be analyzed. In this system, Reconfigurable Optical Add-Drop Multiplexers (ROADMs) represent the nodes and optical fiber the links. ROADMs perform Wavelength Routing (WR) in a transparent way, without needing for Optical-Electrical-Optical (OEO) conversion. A schematic representation of the described network is depicted in Fig.1.17.

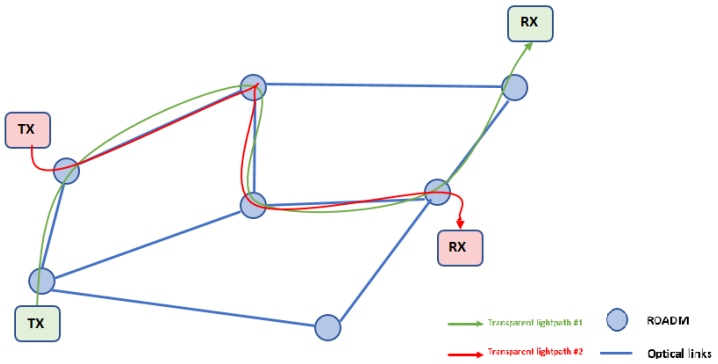

Figure 1.17: Schematic representation of an optical network with ROADM nodes

ROADMs provide the required flexibility thanks to their key component: Wavelength Selective Switching (WSS) which enables remote traffic switching. The main problem of these devices stem the standard WSS transfer function, which is not an ideal rectangle shape in frequency. Thus, if present in a large number, they can act as cascading filters on the signal that is crossing the network, causing non-neglecting penalty, particularly at its edges. Therefore, the goal of this thesis is to introduce a revised WSS transfer function, aiming to minimize this filtering effect as well as improve system performance through different techniques based on Multi-Subcarrier (MSC). The following chapters will focus on the impact of WSS filtering on both Single Carrier (SC) and MSC systems based on both Uniform QAM Constellation and Probabilistic Shaped Constellation (PCS). In case of MSC, additional optimization techniques are analyzed to further improve system performance. The analyzed scenario is characterized by the following parameters:

- 2 signal polarizations
- a fixed net Bit Rate, $R_b = 800$ Gbit/s
- a number of Subcarriers nSC = 16 in MSC case

In addition, Forward Error Correction (FEC) is also implemented to detect and correct error at the receiver, ultimately boosting the overall performance. The original sequence of k bits is then converted into a codeword of n bits by adding n-k redundant bits at the encoding stage before transmission. Thus, the ratio:

$$OH = \frac{n-k}{k} \tag{1.2}$$

is called *Overhead* (OH) and affects the net bit rate. Two different types of FEC have been used during this work: Soft-Decision (SD-FEC) and Hard-Decision (HD-FEC), which are characterized by varying OH and target Bit Error Rate (BER) levels.

This thesis is divided into 4 chapters. Chapter 1 (Introduction) aims to present some fundamentals on the Optical Communications. Chapter 2 presents the model and the impact of filtering of the Standard WSS. Chapter 3 is dedicated to the introduction of the "Bandwidth Enhancement" strategy on WSS filtering with all the simulation results and comparisons with respect to the Standard WSS. Chapter 4 is dedicated to the Conclusion.

Chapter 2

Impact of WSS filtering using Standard WSS

2.1 ROADM

In the early 2000s, optical transport networks' speed increased up to 400 Gb/s, making the electrical switches become inefficient in handling traffic management. To face this problem, ROADM has been introduced, enabling remote switching of wavelengths through the insertion of Wavelength Division Multiplexing (WDM) networks in a transparent way, thus, without needing anymore for Optical-Electrical-Optical (OEO) conversion (Fig. 2.2). Furthermore, according to the number of optical fiber links intersecting at a network node, a degree can be assigned to the ROADMs, with higher degrees providing more routing options and adaptability for complex, large-scale networks. In this work, ROADMs of degree 2 have been considered. They connect 2 fiber links, thus, require 2 WSS, one at the input, needed to select the incoming lightpath, and one at its output, to choose the output lightpath to be routed (Fig. 2.3). In addition, ROADMs introduce other benefits in the optical network, adding to it three important features: *colorless*, *directionless* and *contentionless* [15]. Colorless means that any wavelength can be added or dropped at any port of the ROADM without being restricted to a specific wavelength, thus, improving resource utilization and network flexibility. The term directionless refers to the presence on each transponders of a non-blocking access to any Dense WDM (DWDM) network port within the optical system. In other words this feature allows traffic to be added or dropped at a node in any direction, without being limited to specific fixed path. This eliminates the needs for predetermined paths which, in turn, simplifies route assignments in mesh networks. Contentionless ensures that multiple signals, using the same wavelength, can be added or dropped simultaneously at a node, even if they are directed towards different destinations or directions. Indeed, as the term suggests, it avoids "contention" where signals of the same wavelength would otherwise interfere, enabling more scalable and efficient multi-wavelength operations at each node.
At the heart of ROADM technology lies the WSS which serves as a de/multiplexer of

individual wavelengths to selected common or output ports. A visual representation of this device can be seen in Fig. 2.4. Moreover, there are plenty of technologies that can be used as a WSS switching engine including MEMS (Micro-electromechanical systems), LC (Liquid Crystal) and LCoS (Liquid Crystal on Silicon). The last one is the most used nowadays since it can support flexgrid technology enabled networks, and high port counts with excellent performance [16]. Indeed, also in this work, LCoS based WSS will be considered. The equation modeling the standard WSS filter transfer function is the following:

$$S(f) = \left[\frac{\sigma\sqrt{2\pi}}{2}\left[erf\left(\frac{B/2-f}{\sigma\sqrt{2}}\right) - erf\left(\frac{-B/2-f}{\sigma\sqrt{2}}\right)\right]\right]^{N_{WSS}} \tag{2.1}$$

In 2.1 several variables are introduced: B represents the Bandwidth of the rectangular aperture in frequency, N_{WSS} identifies the number of cascaded WSS present along the line, $\sigma = BW_{OTF}/(\sqrt{2ln2})$ is the standard deviation of the Gaussian shaped Optical Transfer Function (OTF) and BW_{OTF} corresponds to the -3dB bandwidth [17]. Additionally, in this thesis N_{WSS} is an even value and ranges between 0 and 20, or equivalently, a maximum of 10 cascaded ROADMs has been considered.

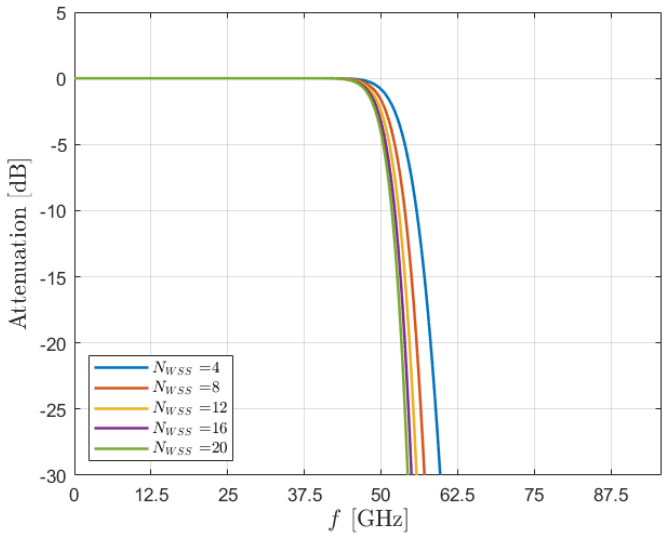

Figure 2.1: Pictorial representation of transfer functions of cascaded WSS given by expression 2.1 where $N_{WSS} \in \{4,..,20\}$ with step=4, B = 134.375 GHz and BW_{OTF} = 10.4 GHz

Observing Fig. 2.1, it can be noticed that as the number of cascaded WSS increases, the transfer function becomes narrower and narrower, penalizing the frequencies at the edges. Moreover, thanks to the simmetricity of this transfer function, only positive

frequencies values have been considered in order to obtain a better graphical visualization of this function, zoomed on the frequency values taken into account.

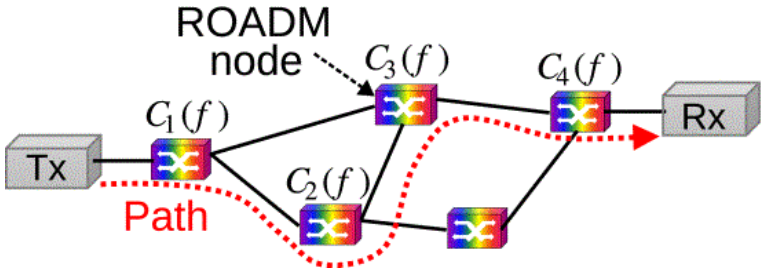

Figure 2.2: Optical network with ROADM nodes, where *C(f)* represents the node's transfer function [18]

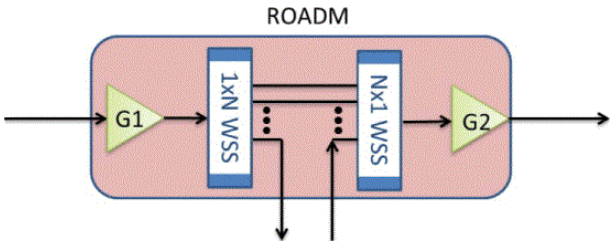

Figure 2.3: Schematic structure of a ROADM node analyzed [19]

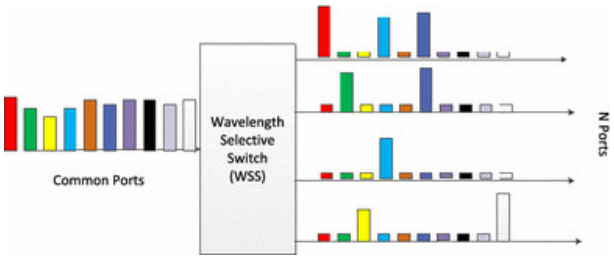

Figure 2.4: Architecture of a Wavelength Selective Switches (WSS) [20]

As discussed in the Introduction, channel modulation can be categorized into Single Carrier (SC) modulation and Multi-Subcarrier (MSC) modulation. In the simulation analysis that will be presented in the next chapters, these approaches are compared to determine if MSC can outperform SC, introducing significative advantages. Currently, to face the increasing capacity requirements, Optical Communication Systems mainly use SC modulation with 2^M-QAM constellations of increasing order M to meet the demands. Fig. 2.5 illustrates the filtering effects on a 128 GBaud SC signal after

passing through 10 cascaded WSS, where the signal's edge frequencies are most affected, though a general decrease in signal quality is noticeable at the receiver. In recent years, with data traffic becoming increasingly diverse, modulation schemes need to be more adaptable and capable of providing finer data-rate granularity. To meet these needs, MSC modulation has gained interest [21] [22]. This approach divides the signal spectrum into N_{SC} subcarriers, each operating at $1/N_{SC}$ of the total symbol rate. Due to she shape of the WSS, filtering effects are more pronounced for the outer subcarriers while, being minimal for those in the center, as shown in Fig.2.6. In this example, DSCM has been exploited to split the original SC signal with a Baud Rate of 128 GBaud into 16 subcarriers each operating at 8 GBaud.

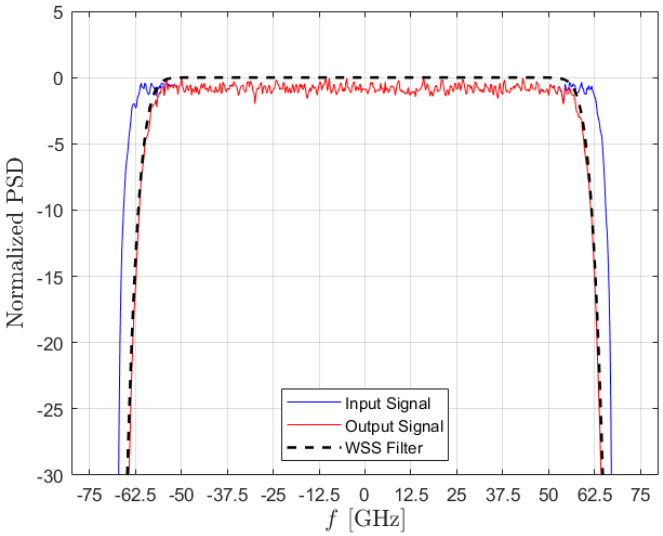

Figure 2.5: Filtering effects on a 128 GBaud SC signal considering 10 cascaded WSSs

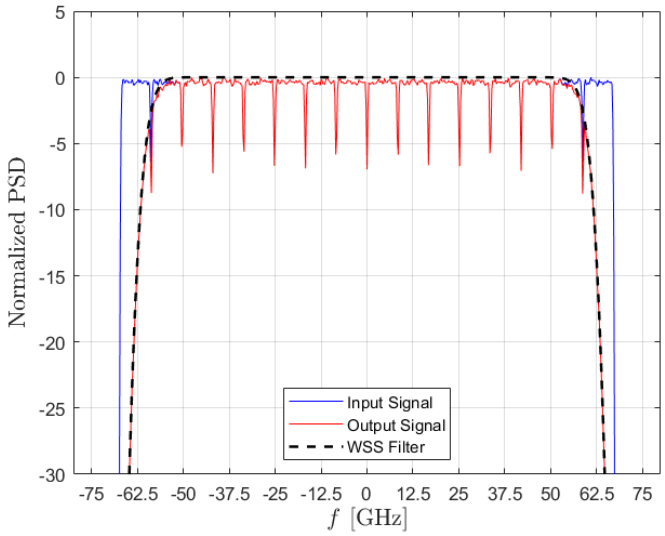

Figure 2.6: Filtering effects on a 128 GBaud 16-MSC signal considering 10 cascaded WSSs

2.2 Optimization Strategies

2.2.1 Useful Definitions

Before starting with the description of the various optimization strategies that can be used, it may be necessary to have a look at a few useful metric and parameters definitions about subcarriers:

- *Signal to Noise Ratio*(SNR) is metric of quality of the transmitted signal. Defined as the ratio between signal's power and the power of the noise floor:

$$SNR = \frac{P_{SIGNAL}}{P_{NOISE}} \tag{2.2}$$

  Usually, it is also computed as a difference between the mentioned quantities when dB is considered as measurement units:

$$SNR_{dB} = P_{SIGNAL_{dBm}} - P_{NOISE_{dBm}} \tag{2.3}$$

- *Power Ratio*(PR) defines the ratio between the Power of the *k-th* subcarrier and the total transmitted power, specifically:

$$PR_k = \frac{P_{SC,k}}{P} \tag{2.4}$$

  As a consequence, $P = \sum_{k=1}^{N_{SC}} P_{SC,k}$

- *SNR* per subcarrier can now be defined as:

$$SNR_k = PR_k \cdot SNR \tag{2.5}$$

- *Bit Error Rate*(BER) its the ratio between the wrongly received bits and the transmitted bits. Furthermore, its value can be computed for each subcarrier as:

$$BER_{SC,k} = \Psi(SNR_{SC,k}, M_k) \tag{2.6}$$

  where Ψ is a non-linear function depending on the geometry of the chosen constellation M_k. Moreover, when squared and cross QAM modulation formats are considered, it can be approximated using the *erfc(·)* function.

With a fixed number of cascaded filters, the attenuation for each subcarrier can be calculated. By subtracting these attenuation values from the channel's SNR, an SNR vector per subcarrier is obtained. This vector is then used by both Uniform QAM Constellation and PCS techniques within their optimization algorithms to improve performance. Optimization strategies are used indeed in order to mitigate filtering effects [23] and they can be firstly classified according the modulation technique for which theywill be used.

2.2.2 Uniform QAM case

Strategies for mitigating filter effects on signals,considering a Uniform QAM Constellation, mainly focus on adjusting either the PR or the modulation format for each subcarrier. They can be classified into:

- *Power Loading (PL)*: this technique aims to compensate for the filtering effect present at the edges of the frequency bandwidth or equivalently on the outer subcarriers. Indeed, using it, lower levels of PR will be obtained for the central subcarriers, while, in contrast higher values for the outer always keeping the same modulation format for each of them.

- *Water Filling (WF)*: using this strategy, more power is allocated on the subcarriers experiencing higher SNR. Thus, the outer subcarriers, the one more penalized by the filtering effect, will receive less power with respect to the inner one.

- *Bit Loading (BL)*: unlike with *PL*, the goal of this strategy is to find the best modulation format for each subcarrier, maintaining the same power. Furthermore, lower-order QAM constellations, are typically assigned to the outer subcarriers due to their higher resilience to channel impairments, such as filtering. Higher-order QAM modulation formats offer higher symbol rates instead, and are generally assigned to the inner subcarriers since they experience a lower filtering effect.

- *Bit and Power Loading (BPL)*: consists in performing both the PL and BL. Thus, both modulation format and power levels are independently adjusted.

The last two optimization strategies are characterized by assigning different modulation formats to each SC, this technique is called Frequency-Domain Hybrid Modulation Formats (FDHMF) and it makes possible to adjust spectral efficiency with fractional granularity, enhancing the tolerance towards filtering caused by ROADM [23]. Moreover, if none of them is applied, there is no power difference between the subcarriers, therefore, $PR_k = 0$ dB for all of them and as a consequence, all subcarriers have the same power and the same modulation format. This scenario is named Same Power&modulation format.

2.2.3 Probabilistic Constellation Shaping case [24]

Another type of modulation technique is the Probabilistic Constellation Shaping(PCS). It is largely used to improve SE and data-rate flexibility.

- *Entropy*, is usually identified with the letter "H". In Uniform QAM case, this value is fixed, depends on the chosen constellation order and it is equal to the number of bits per symbol, according to the following formula:

$$H = \log_2 M \tag{2.7}$$

  In contrast, in PCS this variable doesn't assume a fixed value anymore. Indeed, it is determined by the probability distribution of the source modulator, meaning that a set of input bits are modulated onto the QAM alphabet according to a probability function P(x). Thus the Entropy is now defined as:

$$H(x) = \sum_{i=1}^{M} P(x_i) \log_2 P(x_i) \tag{2.8}$$

- *Capacity* (C) represents the maximum IR supported by the channel and it is independent of the type of modulation. In case of Additive White Gaussian Noise (AWGN) channel, it is computed as:

$$C = \log_2(1 + SNR) \tag{2.9}$$

- *Mutual Information*(MI), quantifies the maximum Achievable Information Rate (AIR) for a given modulation format and channel conditions. Considering 2 discrete random variables X and Y, it can be measured as:

$$I(X;Y) = \sum_{x \in \chi} \sum_{x \in \mathcal{Y}} P_{XY}(x,y) \log \frac{P_{XY}(x,y)}{P_X(x) P_Y(y)} \tag{2.10}$$

  MI offers also information about the useful size of a message and it is counted in units of bits. Indeed, if the entropy is a measure of the uncertainty of a variable X, MI in contrast evaluate the reduction in uncertainty. Thus:

$$MI(X,Y) = H(X) + H(Y) - H(X,Y) \tag{2.11}$$

  where $H(X,Y)$ is the joint entropy of X and Y.

- *Generalized Mutual Information*(GMI) corresponds to the MI when an Additive White Gaussian Noise (AWGN) with Bit Interleaved Coded Modulation is assumed. It can be computed as:

$$GMI = H_{PCS} - G(M_{PCS}, P_x, \sigma^2) \tag{2.12}$$

where G represents the loss of information due to propagation over AWGN channel and is expressed as:

$$G(M_{PCS}, P_x, \sigma^2) = \frac{1}{N}\sum_{n=1}^{N}\sum_{k=1}^{\log_2(M_{PCS})} \log_2 \frac{\sum_{x_m \in \mathcal{X}} \exp\left(-\frac{|y_n - x_m|^2}{\sigma^2}\right) P_{x_m}}{\sum_{x_m \in \mathcal{X}(k, b_{n,k})} \exp\left(-\frac{|y_n - x_m|^2}{\sigma^2}\right) P_{x_m}} \tag{2.13}$$

where σ^2 is the noise variance of the AWGN channel, y_n is the n-th received symbol (on a total of N symbols), x_m is the m-th symbol in the respective constellation alphabet, $b_{n,k}$ is the k-th bit of the n-th transmitted symbol and $\mathcal{X}(k, b)$ indicates a subset of the constellation alphabet, $\mathcal{X}$, which contains bit $b \in [0\ 1]$ in the k-th bit position. Furthermore, the GMI can assume values in a range between 0 and H_{PCS}, which ideally correspond to the worst and best SNR conditions, respectively [25].

- *Normalized Generalized Mutual Information*(NGMI) obtained after proper normalization of GMI, identifies the number of information bits per transmitted bits. Indeed, to provide an universal assessment of achievable information rate for any modulation format, the Normalized GMI (NGMI) is commonly utilized as performance metric and can be defined as:

$$NGMI = 1 - \frac{G(M_{PCS}, P_x, \sigma^2)}{\log_2(M_{PCS}} \tag{2.14}$$

In addition, considering an ideal FEC implementation, it can be proved that the minimum NGMI that ensures error-free transmission is $NGMI_{th} = R_{FEC}$ where R_{FEC} is the FEC rate [25].

PCS lies in assigning different probability to the transmitted symbols as opposed to the Uniform QAM, in which they are all equiprobable. Indeed, this allocation is typically done, through the Distribution Matcher, following the Maxwell-Boltzman (MB) distribution, reported in Eq. 2.15 to form a Gaussian-like constellation.

$$P_{x_n} = \frac{\exp(-\lambda |x_n|^2)}{\sum_{n=1}^{M_{PCS}} \exp(-\lambda |x_n|^2)} \tag{2.15}$$

The Distribution Matcher (DM) is used to shape the transmitted signal's probability distribution. It plays a key role in PCS where it ensures that the symbols are transmitted with non-Uniform probabilities according to the chosen probability distribution. Typically it matches a Gaussian distribution, which improves SE and noise resilience. One of the most used DM is the Constant Composition Distribution Matching (CCDM),

which will be adopted also in this thesis. It is very efficient for PCS since it produces as outputs fixed length sequences of symbols with a set of probabilities distribution, aligning closely with the Maxwell-Boltzmann. For instance, given a $2^M - QAM$ constellation with cardinality 2^M, the probability of each symbol x_n is computed using Eq. 2.15, where the parameter λ is called *Shaping Factor*. It is always greater than or equal to 0 and defines how much the PCS constellation is shaped with respect to the original M_{PCS} one. Specifically, when λ=0, the MB distribution converges to an Uniform one. A pictorial example is shown in Fig. 2.7 where differences between the two approaches becomes noticeable.

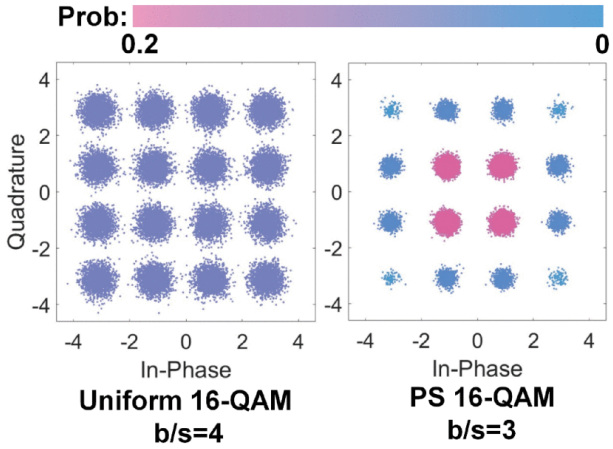

Figure 2.7: Probabilistic shaped 16-QAM and corresponding uniform 16-QAM (b/s: bits/symbol; Prob: Probability) [26]

Entropy Loading [27]

Entropy Loading (EL) in Optical Communication is a technique primarily associated with Probabilistic Constellation Shaping (PCS), used to optimize the data transmission process by controlling the symbol probabilities based on channel conditions. In [27], it was demonstrated that this technique allows to improve the Achievable Information Rate (AIR) by 5% - 10% over BL strategy, using identical FEC OH.
EL is executed ahead of the time-domain simulation, trying to find the optimum λ vector and then pass it to the transmitter. This algorithm follows the steps:

1. The impact of WSS filtering on the subcarriers in terms of SNR level is computed. Thus, given an initial SNR value for the channel, a vector of SNR per subcarrier (SNR_{SC}) is generated as well.

2. Water-Filling (WF) optimization is then performed to obtain new optimized values of SNR_{SC}, grouping them into a new vector $SNR_{WF_{SC}}$. Notice that, the previous

mentioned optimization strategy, basically assigns more power to those subcarriers experiencing higher SNR.

3. In this step it is determined the entropy value for each SNR in the $SNR_{WF_{SC}}$ vector by referencing a Look-Up Table (LUT) generated from Monte-Carlo simulations. The LUT contains the relationships among NGMI, SNR, and entropy, as shown in Fig.2.8. With a target NGMI (i.e at 0.9), the entropy value is identified through an iterative search for the closest match to the given SNR. This process is repeated across all subcarriers, resulting in an output entropy vector H_{SC}.

4. As the final step, a fitting algorithm is applied to the Maxwell-Boltzmann probability distribution to derive a λ value for each H_{SC} value. This process generates the λ_{SC} vector, which is optimized for the initially considered SNR values.

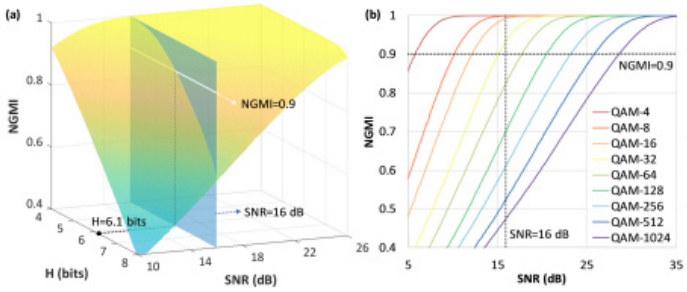

Figure 2.8: Relations between NGMI and SNR (i.e. Look-Up Tables (LUT)) for various modulation formats: (a) PCS 256-QAM; (b) discrete levels of QAM [27].

It is important to notice that in step 3 of the algorithm, conversely with respect to BL, EL can provide a modulation that exactly meets the NGMI target at the specific SNR. BL in contrast cannot reach this task due to the discrete QAM level, and consequently an additional PL should be followed to slightly adjust the SNR for precise NGMI match. Furthermore, also other approaches to the use of the entropy loading have been proposed during years. In [28], a Subcarrier-Pairing Entropy Loading (SubP-EL) has been proposed for digital subcarrier-multiplexed systems exploiting colored SNR distributions, thus, with an SNR's profile that varies across the frequency spectrum, as opposed to a flat SNR where noise is uniformly distributed [28]. In this approach, an iterative optimization of the entropy is performed, always considering subcarrier pairs under a target entropy constraint. After convergence, it has been proved that this algorithm achieves near-optimal performance comparable to brute-force search but with a dramatically reduced complexity. For example, in an 8-subcarrier system with five SNR levels, SubP-EL reduces complexity by factors of 764, 95, and 13 for entropy granularities of 0.05, 0.1, and 0.2 bits/2D-symbol, respectively. Moreover, the results have been experimental validated over 345 km fiber, resulting in an average NGMI gain of 0.0286 over systems without entropy loading, under varying optical filtering conditions.

In addition , EL has been also used to approach the colored-SNR channels paired to the DSCM technique [29]. The jointly use of these techniques has produced relevant benefits in terms of transmission quality in high-rate transmission systems.

Chapter 3

Main Contribution and Simulation Results

In this chapter, the "Bandwidth Enhancement" (BE) technique will be introduced. BE aims to better exploit bandwidth edges to minimize the WSS filtering effect described in Chapter 2. In addition all the simulations' outcomes will also be presented in order to compare all the different optimization strategies introduced in Chapter 2 to counteract the narrowing filtering effects.

3.1 Bandwidth Enhancement [30]

During the years, a number of different solutions have been proposed and implemented to counteract the Bandwidth Narrowing Effect (BNE) as described in Chapter 2. Furthermore, it is also possible to compensate for BNE in the optical domain by spectrally shaping the channel along the transmission path using a Wave Shaper(WS), a device that fine-tunes the spectral shape of the optical signal, adjusting its amplitude or phase across different wavelengths in order to achieve specific filtering effects or signal optimization.
Spectral shaping or Bandwidth Enhancement (BE) is an extremely powerful technique to counteract the WSS filtering effect. To introduce the revised WSS transfer function on which BE relies, some variable have to be described. The transmission window in a LCoS WSS can be described as a rectangular aperture function [17]. For istance:

$$R(f) = \begin{cases} 1, & if - B/2 \leq f \leq +B/2 \\ 0, & otherwhise \end{cases} \tag{3.1}$$

where f is the frequency and B is the channel bandwidth. Furthermore, also the Optical Transfer Function of the WSS has to be introduced. It has a Gaussian shape and it is defined as:

$$L(f) = \frac{1}{\sigma\sqrt{2}} \exp\left[\frac{-f^2}{2\sigma^2}\right] \tag{3.2}$$

It pertains to the 3-dB BW of the OTF by $\sigma = BW_{OTF}/(2\sqrt{2\ln 2})$. Finally, the WSS filter shape is obtained by convoluting the aperture function (Eq.3.1) and the OTF (Eq.3.2):

$$S_A(f) = \frac{1}{2}\left[erf\left(\frac{f+\frac{B}{2}}{\sqrt{2}\sigma}\right) + erf\left(\frac{-f+\frac{B}{2}}{\sqrt{2}\sigma}\right)\right] \tag{3.3}$$

where erf stands for the error function. In the model of the aperture function presented in Eq.3.1, BE is not considered. Indeed, to approximate the increased transmission of the outer slices of the WSS, Dirac delta functions at both ends of the aperture function have been introduced. Thus, the new expression of the numerical aperture becomes:

$$R_{BE}(f) = R(f) + \alpha\sigma\sqrt{2\pi}\delta\left(f+\frac{B}{2}\right) + \alpha\sigma\sqrt{2\pi}\delta\left(f-\frac{B}{2}\right) \tag{3.4}$$

The parameter α is introduced to represent the degree of bandwidth enhancement, where higher values of α correspond to greater enhancement and viceversa. When $\alpha = 0$, no enhancement occurs, and the expression reverts to its original form (Eq.3.1). As before, convolving the aperture function (Eq.3.4) with the OTF transfer function (Eq.3.2) yields an expression for WSS filter shape with the addition of BE.

$$S_B(f) = G\left(f+\frac{B}{2}\right) + G\left(f-\frac{B}{2}\right) \tag{3.5}$$

where

$$G(f) = \frac{1}{2}erf\left(\frac{f}{\sqrt{2}\pi}\right) + \alpha\exp\left(\frac{-f^2}{2\sigma^2}\right) \tag{3.6}$$

When cascaded WSS are considered, the Eq. 3.5 becomes:

$$S_B(f) = \left[G\left(f+\frac{B}{2}\right) + G\left(f-\frac{B}{2}\right)\right]^{N_{WSS}} \tag{3.7}$$

where N_{WSS} indicates the number of cascaded WSS taken into account. Furthermore,as described in [30], an asymmetric version of WSS filter shape can be exploited by assigning different values to the α parameter for each side, thus, obtaining $\alpha_R \neq \alpha_L$ where R stands for "right" and L for "left". For instance Eq.3.5 will become:

$$S_B(f) = G_L\left(f+\frac{B}{2}\right) + G_R\left(f-\frac{B}{2}\right) \tag{3.8}$$

where

$$G(f)_{L,R} = \frac{1}{2}erf\left(\frac{f}{\sqrt{2}\pi}\right) + \alpha_{L,R}\exp\left(\frac{-f^2}{2\sigma^2}\right) \tag{3.9}$$

. In this thesis, only the symmetric case has been considered in which $\alpha_L = \alpha_R = \alpha$.

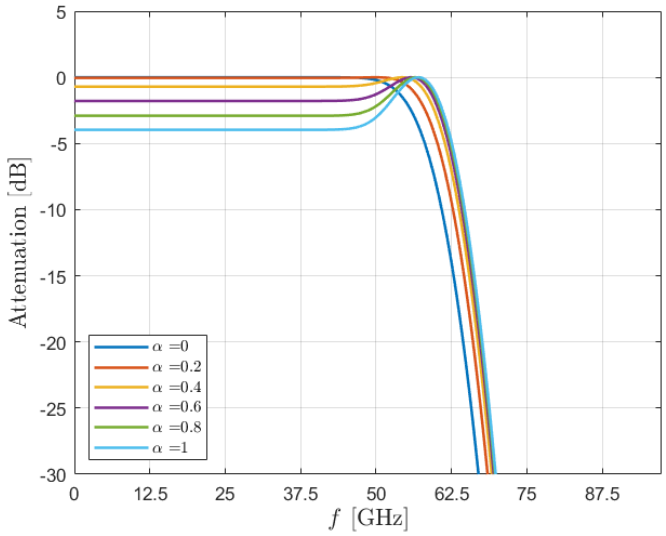

Figure 3.1: Pictorial representation of a single WSS with BE transfer function given by expression 2.1 where $N_{WSS} = 1$, $\alpha \in \{0,..,1\}$ with step=0.2, B = 134.375 GHz and $BW_{OTF} = 10.4$ GHz

In Fig.3.1 a pictorial representation of the WSS transfer function with BE, normalized with respect to its maximum value, is shown.

3.1.1 Optimum alpha evaluation

In BE the parameter α serves to adjust the edges of the WSS filter's transfer function, redistributing energy within the signal's spectrum. On the one hand, increasing its value, frequencies near the filter's cut-off are enhanced, which can counteract the attenuation effects caused by cascaded WSS filtering. This redistribution allows for improved utilization of the available spectrum, particularly at the edges, without altering the overall bandwidth or spectral efficiency. On the other hand, high values of α might introduce performance issues, such as spectral overlap or increased vulnerability to nonlinear effects, which can degrade the overall signal quality. For this reason, its value must be optimized to obtain an optimal trade-off. Indeed, in this thesis simulations also aimed to find, for each considered optimization strategy and number of cascaded WSS, the optimum value of this parameter in order to obtain the best possible performances.

3.2 Detailed Simulated Scenario

Simulations were conducted using MATLAB software, exploiting the OptDSP library, to evaluate system performance as the number of cascaded WSS varies from 0 to 20. In the presented scenario, noise insertion have been performed considering lumped noise at

the receiver side. This assumption means that all WSS filters are combined into a single equivalent filter, followed by the addition of a noise source at the receiver. As a result, the WSS filtering ultimately affects only the signal, leaving the noise level unvaried. This represents a worst-case scenario, as the noise is not mitigated by the filtering process as conversely happen considering it equally distributed among each cascaded WSS.

3.2.1 Forward Error Correction (FEC)

A Forward Error Correction (FEC) technique is employed in the system under test. The parameters of the FEC depend wether Soft-Decision FEC (SD-FEC) and Hard-Decision FEC (HD-FEC) is selected. Their specific values are reported in Table 3.1. For systems using multi-subcarrier modulation, each subcarrier does not employ a separate FEC scheme. Instead, a single FEC is shared across all subcarriers. As a result, the target Bit Error Rate (BER) is compared with the average BER across all subcarriers, in accordance with the system assumptions.
The design of WSS differs significantly between systems employing SD-FEC and HD-FEC, primarly due to the variations in filter bandwidth (B), gross symbol rate, and spectral efficiency (SE), which are influenced by the FEC overhead (FEC OH) and BER target. In SD-FEC systems, WSS filters typically have broader bandwidths to accommodate higer symbol rates and preserve signal quality for effective error correction. As a matter of fact, this is necessary due to higher FEC OH value, which increases the system's ability to correct error but, at the same time, reduces SE by allocating a larger portion of the available bandwidth to redundant data. As a consequence, SD-FEC systems tolerate higher pre-FEC BER compared to HD-FEC systems, which require stricter BER targets due to their lower correction capabilities. Conversely, HD-FEC systems allow narrower filter bandwidths to optimize SE, as the lower FEC OH allows for more efficient use of the available spectrum. However, this come at the cost of reduced error correction capability and a stricter requirement for signal quality at the receiver. Summarizing, SD-FEC prioritizes error tolerance and resilience at the expense of SE. In contrast, HD-FEC emphasizes spectral optimization, requiring higher signal quality and stricter BER.

	SD-FEC	HD-FEC
net Symbol Rate MSC [GBaud]	100	100
gross Symbol Rate MSC [GBaud]	128	112
FEC OH	0.20	0.07
Total OH	0.28	0.12
BER Target	$2.4{\cdot}10^{-2}$	$3.8{\cdot}10^{-3}$
WSS Bandwidth [GHz]	134.375	117.580

Table 3.1: Simulation parameters for SD-FEC and HD-FEC

3.2.2 WSS filter modeling

In the conducted simulations, the WSS filter was modeled using an analytical representation of its revisited transfer function, as detailed in Eq. 3.7. The number of cascaded WSS considered in the simulations, denoted as N_{WSS}, ranged from 0 to 20 in increments of 2. When the WSS with BE is considered, the parameter α which actually denotes the intensity of BE, was first varied between 0 and 1 and then a fine tuning has been done between 0 and 0.35 with different resolutions depending on the considered constellation. Specifically, a resolution of 0.01 was applied with the Uniform QAM constellation, while a resolution of 0.02 in case of PCS. The bandwidth parameter B was set to either equal to 134.375 GHz or 117.580 GHz depending on the FEC type considered, SD-FEC or HD-FEC, respectively. The optical filter bandwidth BW_{OTF} represents the bandwidth of the filter's transfer function and was set to 10.4 GHz.

3.3 Simulation Results using different techniques

3.3.1 BER and GMI target

After the conclusion of each time-domain simulation, transmission performance are evaluated. To make it possible, 2 different metrics have been adopted, according to the constellation type considered. For istance, in case of Uniform QAM constellations, BER has been used, while for PSC, GMI has been chosen. These metrics offer different approaches for assessing transmission quality. Both methods enable the determination of the minimum SNR required to reach the target values.

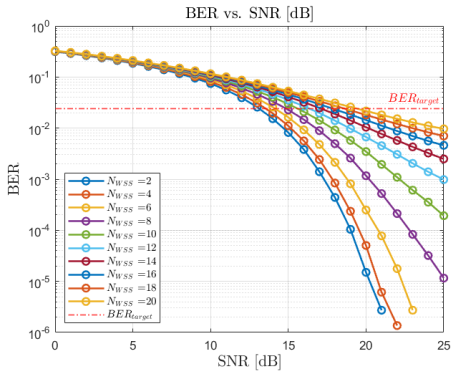

Figure 3.2: BER vs. SNR [dB] for a SC SD-FEC considering $\alpha = 0$ and $N_{WSS} \in \{2,..,20\}$

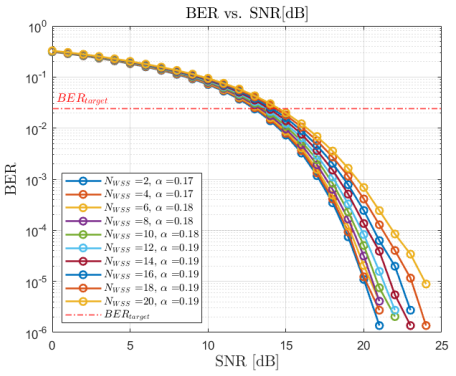

Figure 3.3: BER vs. SNR [dB] for a SC SD-FEC considering $\alpha = \alpha_{opt.}$ and $N_{WSS} \in \{2,..,20\}$

A Single-Carrier(SC) system, as simplest example, utilizing the standard WSS ($\alpha = 0$) and SD-FEC has been analyzed. In Fig.3.2, it can be observed that the required SNR to achieve the target BER increases with the number of cascaded WSS units considered.

This trend underscores the degradation introduced as additional filtering stages accumulate. However, Fig.3.3 illustrates a significant improvement in performance. Specifically, the required SNR values decrease dramatically when an optimal value for the parameter α is considered for each N_{WSS} value, as opposed to the standard value $\alpha = 0$. This result highlights the benefit of α optimization in mitigating SNR penalties when cascaded WSS are involved. The same process has been used in PCS case to extrapolate the minimum value of SNR [dB] required to reach the target value. Thus, it has been only changed the performance metric to be evaluated from BER to GMI setting a target value GMI = 3.33 [bits/sym].

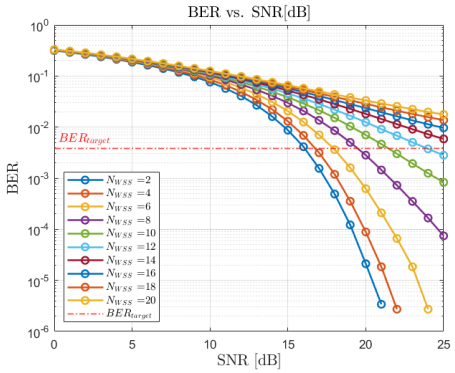

Figure 3.4: BER vs. SNR [dB] for a SC HD-FEC considering $\alpha = 0$ and $N_{WSS} \in$ {2,..,20}

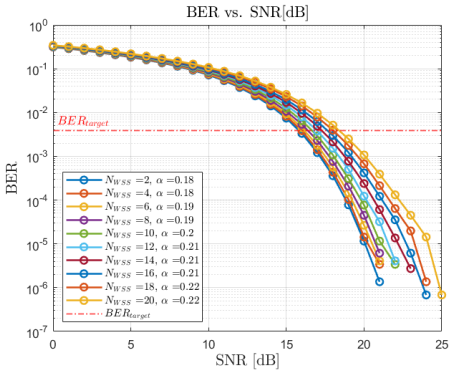

Figure 3.5: BER vs. SNR [dB] for a SC HD-FEC considering $\alpha = \alpha_{opt.}$ and $N_{WSS} \in$ {2,..,20}

The same trend is also observed when considering the HD-FEC case of the same system. Furthermore, looking at Fig.3.4 a noticeable limitation of mantaining $\alpha = 0$ can be take out. Indeed, it is possible to note that, starting from N_{WSS}=14, the required SNR at the target BER would be too high, resulting in unreasonable values. Fig.3.5 illustrates the trend when the optimal α for the different number of cascaded WSS (N_{WSS}) value is applied. As shown, in this case, in all the examined cascaded N_{WSS} scenarios the target BER, with acceptable SNR values, is achieved. This finding definitively proves the effectiveness of α optimization in ensuring system performance even under demanding conditions.

3.4 Uniform QAM comparison

In the next sections, two different systems will be analyzed and compared: Single Carrier (SC) systems and Multi-Subcarrier (MSC) systems. The implementation of MSC systems is enabled by Subcarrier Multiplexing (SCM), which is performed through DSP. SCM is an effective solution to mitigate the filtering effects introduced by WSS. By dividing the signal into N_{SC} subcarriers allowing for various optimization strategies such as: BL, PL, BPL and WF which have been introduced in sect. 2.2. Moreover, this

technique can be employed either as a stand-alone approach or in conjunction with BE, where the parameter α is optimized. However, in the SC systems, only α optimization can be performed, since the signal in this case is transmitted as a single entity, thus without the possibility to manipulate independently each subcarrier. The graphical results of these approaches will be presented and compared in the subsequent sections of this chapter.

3.4.1 Same Power

Starting from the baseline scenario where all subcarriers are assigned same power and employ the same modulation format (i.e. 16-QAM), notable observations regarding the minimum required SNR to achieve the target BER are presented in the following figures. These results serve as a benchmark for understanding the performance limits of the standard WSS under demanding system conditions.

Single Carrier (SC) case

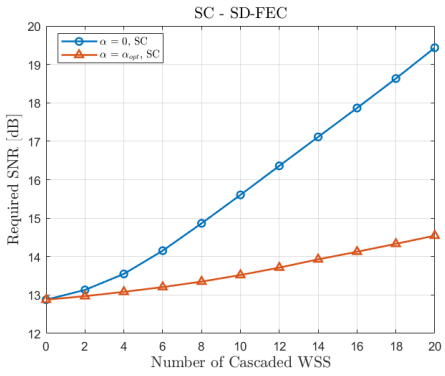

Figure 3.6: Required SNR [dB] vs. N_{WSS} with $\alpha = 0$ and $\alpha = \alpha_{opt}$ for $N_{WSS} \in \{0,..,20\}$, SC SD-FEC

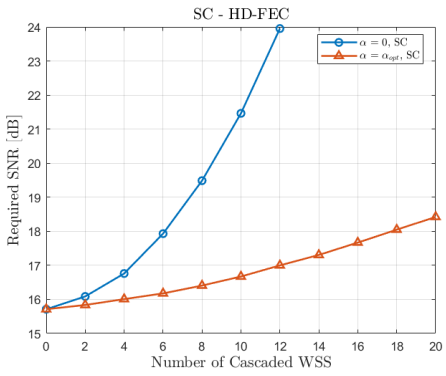

Figure 3.7: Required SNR [dB] vs. N_{WSS} with $\alpha = 0$ and $\alpha = \alpha_{opt}$ for $N_{WSS} \in \{0,..,20\}$, SC HD-FEC

As previously discussed and illustrated in Fig. 3.4, SC systems using HD-FEC are unable to reach the target BER, with an SNR up to 25 dB, when a cascaded number beyond $N_{WSS} = 14$ and $\alpha = 0$ are considered. However, Fig. 3.7 demonstrates that this limitation is resolved for $\alpha \neq 0$. Furthermore, by optimizing the α parameter and selecting its value corresponding to the minimum SNR point on the curve plotted in Fig.3.8, the system not only overcomes this constraint but also achieves an optimal solution in terms of required SNR.

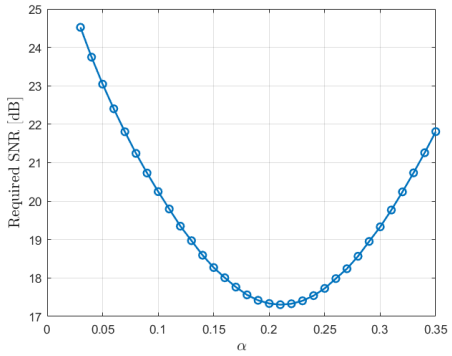

Figure 3.8: Required SNR [dB] vs. α for $N_{WSS} = 14$, SC HD-FEC

Multi Subcarrier (MSC) case

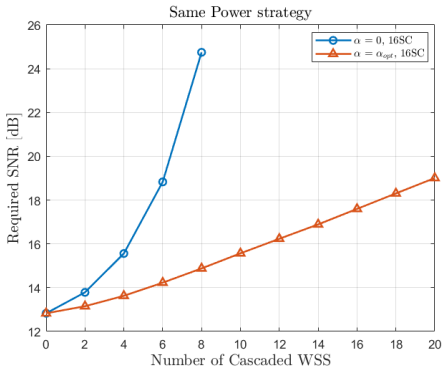

Figure 3.9: Required SNR [dB] vs. N_{WSS} with $\alpha = 0$ and $\alpha = \alpha_{opt}$ for $N_{WSS} \in \{0,..,20\}$, 16SCs SD-FEC , Same Power strategy

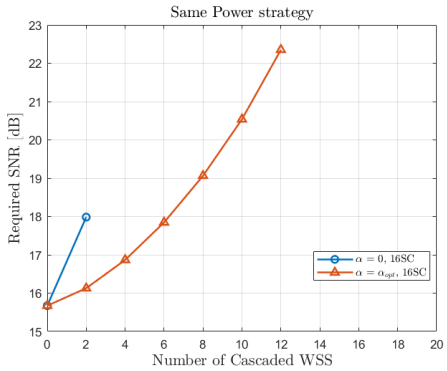

Figure 3.10: Required SNR [dB] vs. N_{WSS} with $\alpha = 0$ and $\alpha = \alpha_{opt}$ for $N_{WSS} \in \{0,..,20\}$, 16SCs HD-FEC , Same Power strategy

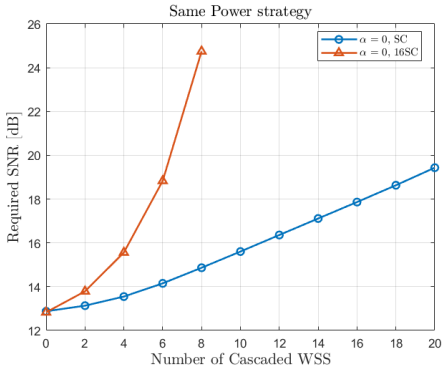

Figure 3.11: Required SNR [dB] vs. N_{WSS} with $\alpha = 0$ SC and $\alpha = 0$ 16SCs for $N_{WSS} \in \{0,..,20\}$, SD-FEC, Same Power strategy

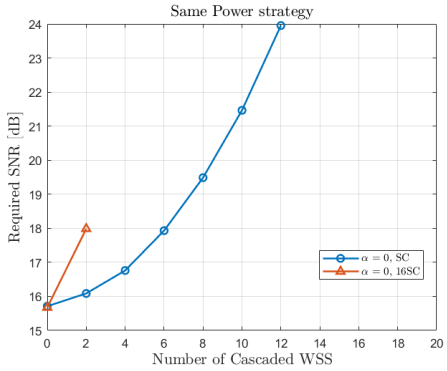

Figure 3.12: Required SNR [dB] vs. N_{WSS} with $\alpha = 0$ SC and $\alpha = 0$ 16SCs for $N_{WSS} \in \{0,..,20\}$, HD-FEC, Same Power strategy

Extending the same power strategy to the MSC case, the results in Figg. 3.9 to 3.14 are obtained. Looking at Fig.3.9 and Fig.3.10, it is straightforward to notice that adopting an optimum alpha value for each N_{WSS} considered, significantly enhances the performance. Furthermore, it is also clearly revealed that unreasonable SNR values are obtained for N_{WSS} beyond 2 when α =0 and HD-FEC are considered. Another observation that can be done, regards the comparison between the SC and MSCs case. Specifically when HD-FEC and α =0 are involved. Indeed, in Fig.3.12 it is noticeable that SC system outperforms MSC one in this case. This outcome arises from the fact that when MSC

with Same Power are considered, the overall power of the signal is sliced in N_{SC} equal parts per subcarriers, thus, if the filtering effects are severe, the outer subcarriers are almost entirely lost, consequently loosing a lot of carried power and information. This underscores the importance of proper power allocation and optimization in MSCs system.

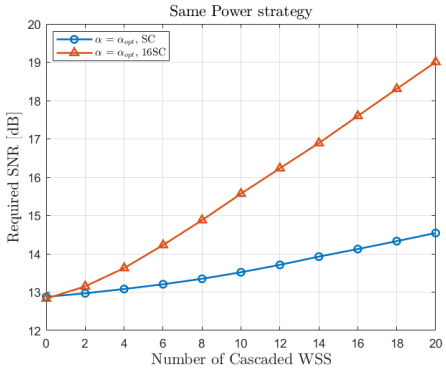

Figure 3.13: Required SNR [dB] vs. N_{WSS} with $\alpha = \alpha_{opt}$ SC and $\alpha = \alpha_{opt}$ 16SCs for $N_{WSS} \in \{0,..,20\}$, SD-FEC, Same Power strategy

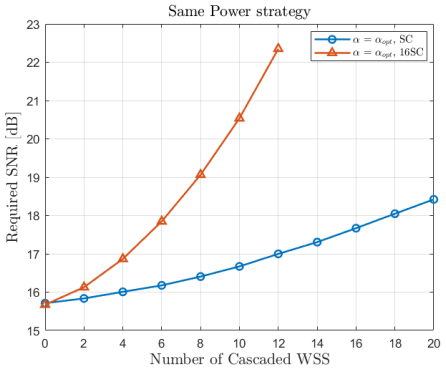

Figure 3.14: Required SNR [dB] vs. N_{WSS} with $\alpha = \alpha_{opt}$ SC and $\alpha = \alpha_{opt}$ 16SCs for $N_{WSS} \in \{0,..,20\}$, HD-FEC, Same Power strategy

3.4.2 Bit Loading

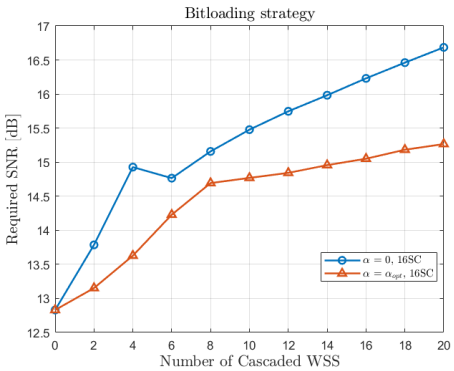

Figure 3.15: Required SNR [dB] vs. N_{WSS} with $\alpha = 0$ and $\alpha = \alpha_{opt}$ for $N_{WSS} \in \{0,..,20\}$, 16SCs SD-FEC , Bit Loading strategy

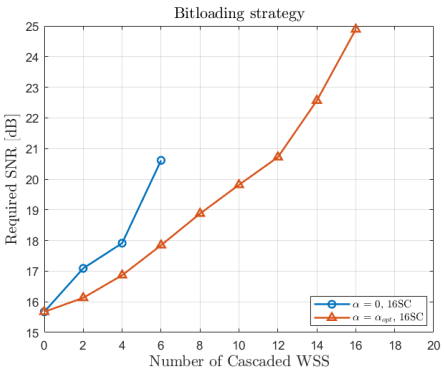

Figure 3.16: Required SNR [dB] vs. N_{WSS} with $\alpha = 0$ and $\alpha = \alpha_{opt}$ for $N_{WSS} \in \{0,..,20\}$, 16SCs HD-FEC , Bit Loading strategy

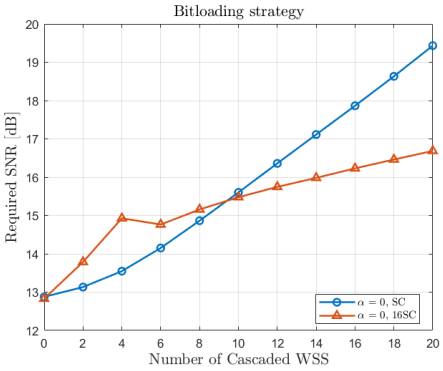

Figure 3.17: Required SNR [dB] vs. N_{WSS} with $\alpha = 0$ SC and $\alpha = 0$ 16SCs for $N_{WSS} \in \{0,..,20\}$, SD-FEC, Bit Loading strategy

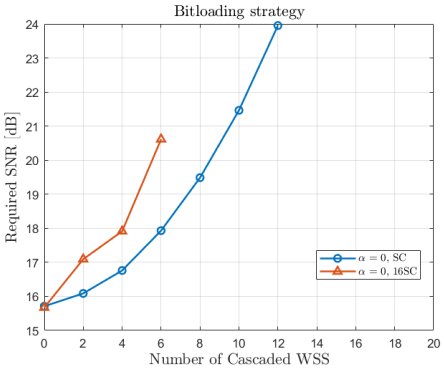

Figure 3.18: Required SNR [dB] vs. N_{WSS} with $\alpha = 0$ SC and $\alpha = 0$ 16SCs for $N_{WSS} \in \{0,..,20\}$, HD-FEC, Bit Loading strategy

In this case, the Bit Loading technique was utilized to allocate different modulation formats to subcarriers according to the filtering effects they experienced. Generally, subcarriers located at the edges of the frequency bandwidth are assigned lower modulation formats, while central subcarriers are allocated higher ones (Sect.2.2). This allocation pattern is reflected in Table 3.2, showing the modulation formats across subcarriers under different numbers of cascaded WSS with α set to 0. The implementation of BE led to significant performance improvements, as demonstrated in Table 3.3. Using the optimal value for α equal to α_{opt} across multiple WSS cases allowed each subcarrier

to operate at a uniform modulation format up to 6 cascaded WSS, effectively overcoming to the impact of filtering. This dual optimization approach, involving fine-tuning of α and modulation format allocation, brought to a significant enhancement in system performance, ultimately enabling more efficient utilization of the entire bandwidth. Furthermore, as shown in Fig.3.17, it can be observed that this technique, when an SD-FEC scenario without BE is considered, outperforms the SC system. Specifically, it requires a lower SNR to achieve the target BER when the number of cascaded WSS lies between 10 and 20. This underscores another time, the intrinsic efficiency of the MSC systems under such conditions, highlighting their robustness against filtering effects compared to the SCs counterpart.

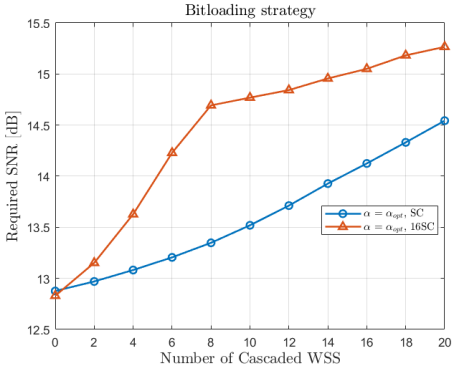

Figure 3.19: Required SNR [dB] vs. N_{WSS} with $\alpha = \alpha_{opt}$ SC and $\alpha = \alpha_{opt}$ 16SCs for $N_{WSS} \in \{0,..,20\}$, SD-FEC, Bit Loading strategy

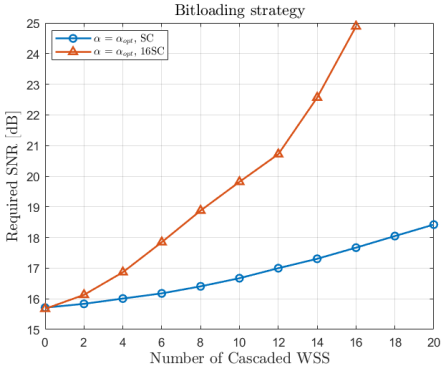

Figure 3.20: Required SNR [dB] vs. N_{WSS} with $\alpha = \alpha_{opt}$ SC and $\alpha = \alpha_{opt}$ 16SCs for $N_{WSS} \in \{0,..,20\}$, HD-FEC, Bit Loading strategy

Modulation format per SC																
	SC 1	SC 2	SC 3	SC 4	SC 5	SC 6	SC 7	SC 8	SC 9	SC 10	SC 11	SC 12	SC 13	SC 14	SC 15	SC 16
0 WSS	16	16	16	16	16	16	16	16	16	16	16	16	16	16	16	16
2 WSS	16	16	16	16	16	16	16	16	16	16	16	16	16	16	16	16
4 WSS	8	16	16	16	16	16	16	32	32	16	16	16	16	16	16	8
6 WSS	4	16	16	16	16	16	32	32	32	32	16	16	16	16	16	4
8 WSS	4	16	16	16	16	16	32	32	32	32	16	16	16	16	16	4
10 WSS	4	16	16	16	16	16	32	32	32	32	16	16	16	16	16	4
12 WSS	4	16	16	16	16	16	32	32	32	32	16	16	16	16	16	4
14 WSS	4	16	16	16	16	16	32	32	32	32	16	16	16	16	16	4
16 WSS	4	16	16	16	16	16	32	32	32	32	16	16	16	16	16	4
18 WSS	4	16	16	16	16	16	32	32	32	32	16	16	16	16	16	4
20 WSS	4	16	16	16	16	16	32	32	32	32	16	16	16	16	16	4

Table 3.2: Modulation formats per subcarrier using Bit Loading strategy with $\alpha = 0$ and SNR[dB] = required SNR at $\alpha = 0$ for $N_{WSS} \in \{0,..,20\}$, SD-FEC

Modulation format per SC																
	SC 1	SC 2	SC 3	SC 4	SC 5	SC 6	SC 7	SC 8	SC 9	SC 10	SC 11	SC 12	SC 13	SC 14	SC 15	SC 16
0 WSS	16	16	16	16	16	16	16	16	16	16	16	16	16	16	16	16
2 WSS	16	16	16	16	16	16	16	16	16	16	16	16	16	16	16	16
4 WSS	16	16	16	16	16	16	16	16	16	16	16	16	16	16	16	16
6 WSS	16	16	16	16	16	16	16	16	16	16	16	16	16	16	16	16
8 WSS	4	16	16	16	16	16	32	32	32	32	16	16	16	16	16	4
10 WSS	4	16	16	16	16	16	32	32	32	32	16	16	16	16	16	4
12 WSS	4	16	16	16	16	16	32	32	32	32	16	16	16	16	16	4
14 WSS	4	16	16	16	16	16	32	32	32	32	16	16	16	16	16	4
16 WSS	4	16	16	16	16	16	32	32	32	32	16	16	16	16	16	4
18 WSS	4	16	16	16	16	16	32	32	32	32	16	16	16	16	16	4
20 WSS	4	16	16	16	16	16	32	32	32	32	16	16	16	16	16	4

Table 3.3: Modulation formats per subcarrier using Bit Loading strategy with $\alpha = \alpha_{opt}$ and SNR[dB] = required SNR at α_{opt} for $N_{WSS} \in \{0,..,20\}$, SD-FEC

3.4.3 Power Loading

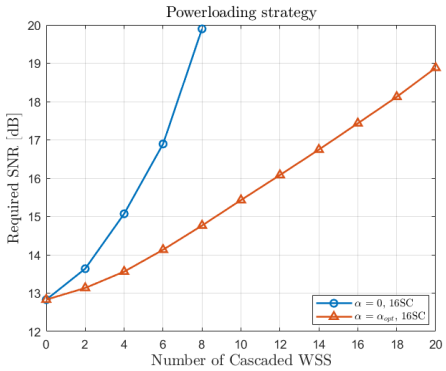

Figure 3.21: Required SNR [dB] vs. N_{WSS} with $\alpha = 0$ and $\alpha = \alpha_{opt}$ for $N_{WSS} \in \{0,..,20\}$, 16SCs SD-FEC , Power Loading strategy

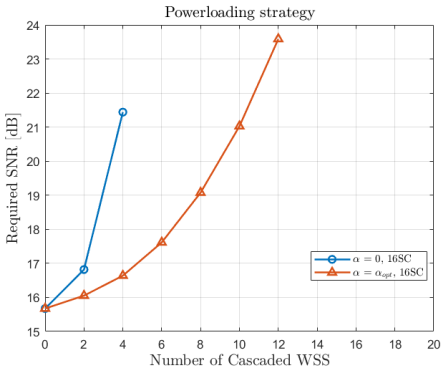

Figure 3.22: Required SNR [dB] vs. N_{WSS} with $\alpha = 0$ and $\alpha = \alpha_{opt}$ for $N_{WSS} \in \{0,..,20\}$, 16SCs HD-FEC , Power Loading strategy

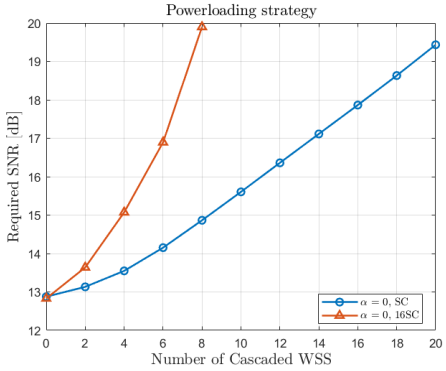

Figure 3.23: Required SNR [dB] vs. N_{WSS} with $\alpha = 0$ SC and $\alpha = 0$ 16SCs for $N_{WSS} \in \{0,..,20\}$, SD-FEC, Power Loading strategy

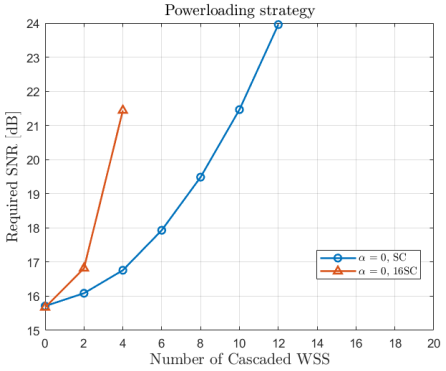

Figure 3.24: Required SNR [dB] vs. N_{WSS} with $\alpha = 0$ SC and $\alpha = 0$ 16SCs for $N_{WSS} \in \{0,..,20\}$, HD-FEC, Power Loading strategy

In this case, the Power Loading technique was exploited to allocate different power levels to subcarriers according to the filtering effects they encountered. As already seen, subcarriers located at the edges of the frequency bandwidth are more affected from filtering effects when $\alpha = 0$ is considered. Thus, high power levels are assigned to counteract the narrowing effect, conversely with respect to the central subcarriers where less power is needed according to what has been previously defined into Sect.2.2. This allocation scheme is reported in Tables 3.4 and 3.6, showing the different power ratios, measured in dB, assigned to each subcarrier under different numbers of cascaded

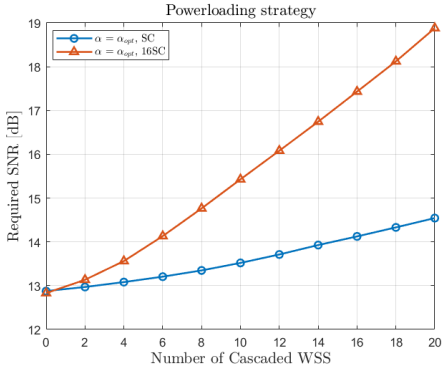

Figure 3.25: Required SNR [dB] vs. N_{WSS} with $\alpha = \alpha_{opt}$ SC and $\alpha = \alpha_{opt}$ 16SCs for $N_{WSS} \in \{0,..,20\}$, SD-FEC, Power Loading strategy

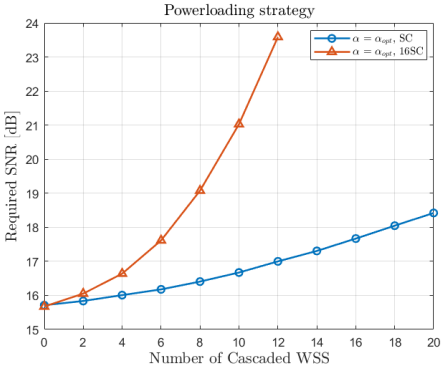

Figure 3.26: Required SNR [dB] vs. N_{WSS} with $\alpha = \alpha_{opt}$ SC and $\alpha = \alpha_{opt}$ 16SCs for $N_{WSS} \in \{0,..,20\}$, HD-FEC, Power Loading strategy

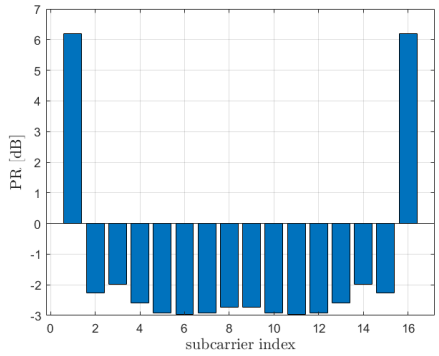

Figure 3.27: Pictorial representation of Power Ratios per subcarrier using Power Loading strategy with $\alpha = 0$, SNR[dB] = 25, $N_{WSS} = 10$, SD-FEC

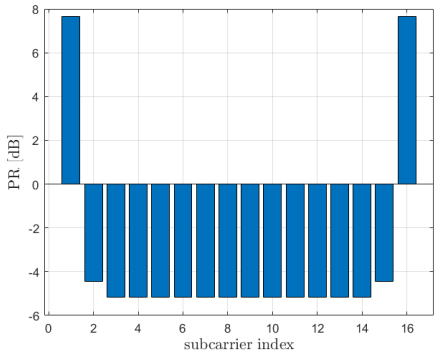

Figure 3.28: Pictorial representation of Power Ratios per subcarrier using Power Loading strategy with $\alpha = 0$, SNR[dB] = 25, $N_{WSS} = 20$, SD-FEC

WSS. However, the implementation of BE, modifies the actual shape of the WSS's filter transfer function and, as a consequence, also the power ratios changes as demonstrated in Tables 3.5 and 3.7. For instance, using a value of α equal to 0.33 in HD-FEC scenario, leads to a lower need in terms of allocated power on the outer subcarriers. Although, as it can be noticed in Figg. 3.27 - 3.30, an higher power compensation is required on the inner subcarriers. This behavior leads to a trade off between the increasing of spectral efficiency and the attenuation experienced by the subcarriers across multiple WSS cases.

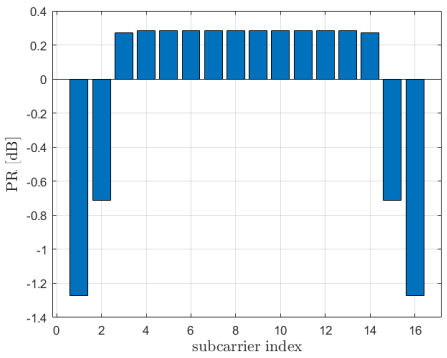

Figure 3.29: Pictorial representation of Power Ratios per subcarrier using Power Loading strategy with $\alpha = 0.33$, SNR[dB] = 25, $N_{WSS} = 10$, HD-FEC

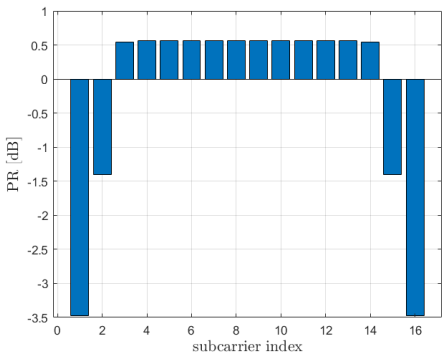

Figure 3.30: Pictorial representation of Power Ratios per subcarrier using Power Loading strategy with $\alpha = 0.33$, SNR[dB] = 25, $N_{WSS} = 20$, HD-FEC

Power Ratios per SC																
	SC 1	SC 2	SC 3	SC 4	SC 5	SC 6	SC 7	SC 8	SC 9	SC 10	SC 11	SC 12	SC 13	SC 14	SC 15	SC 16
0 WSS	0	0	0	0	0	0	0	0	0	0	0	0	0	0	0	0
2 WSS	1.6636	-0.2481	-0.3082	-0.3087	-0.3082	-0.3083	-0.3084	-0.3084	-0.3084	-0.3084	-0.3083	-0.3082	-0.3087	-0.3082	-0.2481	1.6636
4 WSS	2.7811	-0.4874	-0.6139	-0.6142	-0.6139	-0.6140	-0.6140	-0.6140	-0.6140	-0.6140	-0.6140	-0.6139	-0.6142	-0.6139	-0.4874	2.7811
6 WSS	4.0002	-0.8786	-1.0870	-1.0874	-1.0871	-1.0875	-1.0873	-1.0872	-1.0872	-1.0873	-1.0875	-1.0871	-1.0874	-1.0870	-0.8786	4.0002
8 WSS	5.2134	-1.4900	-1.7946	-1.7949	-1.7949	-1.7949	-1.7949	-1.7950	-1.7950	-1.7949	-1.7949	-1.7949	-1.7949	-1.7946	-1.4900	5.2134
10 WSS	-9.9901	0.4519	0.5373	0.5374	0.5373	0.5372	0.5373	0.5371	0.5371	0.5373	0.5372	0.5373	0.5374	0.5373	0.4519	-9.9901
12 WSS	-11.1329	0.4488	0.5524	0.5527	0.5526	0.5526	0.5524	0.5527	0.5527	0.5524	0.5526	0.5526	0.5527	0.5524	0.4488	-11.1329
14 WSS	-12.1830	0.4416	0.5641	0.5644	0.5641	0.5643	0.5644	0.5643	0.5643	0.5644	0.5643	0.5641	0.5644	0.5641	0.4416	-12.1830
16 WSS	-13.1691	0.4314	0.5735	0.5738	0.5737	0.5738	0.5738	0.5738	0.5738	0.5738	0.5738	0.5737	0.5738	0.5735	0.4314	-13.1691
18 WSS	-14.1084	0.4190	0.5816	0.5817	0.5818	0.5815	0.5815	0.5818	0.5818	0.5815	0.5815	0.5818	0.5817	0.5816	0.4190	-14.1084
20 WSS	-15.0121	0.4055	0.5882	0.5886	0.5887	0.5884	0.5884	0.5884	0.5884	0.5884	0.5884	0.5887	0.5886	0.5882	0.4055	-15.0121

Table 3.4: Power Ratios per subcarrier using Power Loading strategy with $\alpha = 0$ and SNR[dB] = required SNR at $\alpha = 0$ for $N_{WSS} \in \{0,..,20\}$, SD-FEC

Power Ratios per SC																
	SC 1	SC 2	SC 3	SC 4	SC 5	SC 6	SC 7	SC 8	SC 9	SC 10	SC 11	SC 12	SC 13	SC 14	SC 15	SC 16
0 WSS	0	0	0	0	0	0	0	0	0	0	0	0	0	0	0	0
2 WSS	0.6380	-0.1115	-0.0974	-0.0971	-0.0974	-0.0971	-0.0974	-0.0973	-0.0973	-0.0974	-0.0971	-0.0974	-0.0971	-0.0974	-0.1115	0.6380
4 WSS	0.9695	-0.1983	-0.1515	-0.1513	-0.1514	-0.1512	-0.1512	-0.1515	-0.1515	-0.1512	-0.1512	-0.1514	-0.1513	-0.1515	-0.1983	0.9695
6 WSS	1.0633	-0.2457	-0.1645	-0.1641	-0.1639	-0.1641	-0.1637	-0.1640	-0.1640	-0.1637	-0.1641	-0.1639	-0.1641	-0.1645	-0.2457	1.0633
8 WSS	1.3219	-0.3280	-0.2104	-0.2097	-0.2098	-0.2098	-0.2098	-0.2098	-0.2098	-0.2098	-0.2098	-0.2098	-0.2097	-0.2104	-0.3280	1.3219
10 WSS	1.2018	-0.3454	-0.1794	-0.1793	-0.1787	-0.1792	-0.1790	-0.1789	-0.1789	-0.1790	-0.1792	-0.1787	-0.1793	-0.1794	-0.3454	1.2018
12 WSS	1.3544	-0.4183	-0.2040	-0.2029	-0.2029	-0.2029	-0.2032	-0.2027	-0.2027	-0.2032	-0.2029	-0.2029	-0.2029	-0.2040	-0.4183	1.3544
14 WSS	1.4779	-0.4893	-0.2229	-0.2217	-0.2216	-0.2218	-0.2216	-0.2216	-0.2216	-0.2216	-0.2218	-0.2216	-0.2217	-0.2229	-0.4893	1.4779
16 WSS	1.1365	-0.4822	-0.1437	-0.1426	-0.1424	-0.1426	-0.1427	-0.1426	-0.1426	-0.1427	-0.1426	-0.1424	-0.1426	-0.1437	-0.4822	1.1365
18 WSS	1.1714	-0.5451	-0.1424	-0.1407	-0.1407	-0.1410	-0.1406	-0.1405	-0.1405	-0.1406	-0.1410	-0.1407	-0.1407	-0.1424	-0.5451	1.1714
20 WSS	0.7330	-0.5645	-0.0466	-0.0447	-0.0446	-0.0447	-0.0449	-0.0449	-0.0449	-0.0449	-0.0447	-0.0446	-0.0447	-0.0466	-0.5645	0.7330

Table 3.5: Power Ratios per subcarrier using Power Loading strategy with $\alpha = \alpha_{opt}$ and SNR[dB] = required SNR at α_{opt} for $N_{WSS} \in \{0,..,20\}$, SD-FEC

Power Ratios per SC																
	SC 1	SC 2	SC 3	SC 4	SC 5	SC 6	SC 7	SC 8	SC 9	SC 10	SC 11	SC 12	SC 13	SC 14	SC 15	SC 16
0 WSS	0	0	0	0	0	0	0	0	0	0	0	0	0	0	0	0
2 WSS	2.4533	-0.3654	-0.5205	-0.5215	-0.5215	-0.5215	-0.5212	-0.5212	-0.5212	-0.5212	-0.5215	-0.5215	-0.5215	-0.5205	-0.3654	2.4533
4 WSS	4.4283	-0.9760	-1.3167	-1.3188	-1.3187	-1.3187	-1.3187	-1.3188	-1.3188	-1.3187	-1.3187	-1.3187	-1.3188	-1.3167	-0.9760	4.4283
6 WSS	-8.8999	0.4085	0.5256	0.5260	0.5261	0.5261	0.5260	0.5262	0.5262	0.5260	0.5261	0.5261	0.5260	0.5256	0.4085	-8.8999
8 WSS	-10.7936	0.3949	0.5567	0.5574	0.5575	0.5575	0.5573	0.5574	0.5574	0.5573	0.5575	0.5575	0.5574	0.5567	0.3949	-10.7936
10 WSS	-12.4553	0.3670	0.5779	0.5786	0.5787	0.5788	0.5787	0.5787	0.5787	0.5787	0.5788	0.5787	0.5786	0.5779	0.3670	-12.4553
12 WSS	-13.9809	0.3308	0.5944	0.5952	0.5951	0.5949	0.5950	0.5949	0.5949	0.5950	0.5949	0.5951	0.5952	0.5944	0.3308	-13.9809
14 WSS	-15.4192	0.2886	0.6077	0.6089	0.6089	0.6086	0.6089	0.6087	0.6087	0.6089	0.6086	0.6089	0.6089	0.6077	0.2886	-15.4192
16 WSS	-16.7938	0.2420	0.6197	0.6207	0.6208	0.6208	0.6210	0.6210	0.6210	0.6210	0.6208	0.6208	0.6207	0.6197	0.2420	-16.7938
18 WSS	-18.1189	0.1913	0.6307	0.6320	0.6320	0.6320	0.6320	0.6321	0.6321	0.6320	0.6320	0.6320	0.6320	0.6307	0.1913	-18.1189
20 WSS	-19.4097	0.1376	0.6411	0.6425	0.6427	0.6426	0.6423	0.6427	0.6427	0.6423	0.6426	0.6427	0.6425	0.6411	0.1376	-19.4097

Table 3.6: Power Ratios per subcarrier using Power Loading strategy with $\alpha = 0$ and SNR[dB] = required SNR at $\alpha = 0$ for $N_{WSS} \in \{0,..,20\}$, HD-FEC

Power Ratios per SC																
	SC 1	SC 2	SC 3	SC 4	SC 5	SC 6	SC 7	SC 8	SC 9	SC 10	SC 11	SC 12	SC 13	SC 14	SC 15	SC 16
0 WSS	0	0	0	0	0	0	0	0	0	0	0	0	0	0	0	0
2 WSS	0.9307	-0.1791	-0.1467	-0.1461	-0.1461	-0.1462	-0.1459	-0.1461	-0.1461	-0.1459	-0.1462	-0.1461	-0.1461	-0.1467	-0.1791	0.9307
4 WSS	1.2201	-0.3151	-0.1900	-0.1880	-0.1878	-0.1879	-0.1876	-0.1878	-0.1878	-0.1876	-0.1879	-0.1878	-0.1880	-0.1900	-0.3151	1.2201
6 WSS	1.0053	-0.4126	-0.1278	-0.1241	-0.1242	-0.1241	-0.1243	-0.1236	-0.1236	-0.1243	-0.1241	-0.1242	-0.1241	-0.1278	-0.4126	1.0053
8 WSS	0.0658	-0.4899	0.0601	0.0669	0.0668	0.0667	0.0668	0.0667	0.0667	0.0668	0.0667	0.0668	0.0669	0.0601	-0.4899	0.0658
10 WSS	-1.1398	-0.6346	0.2495	0.2594	0.2594	0.2593	0.2593	0.2592	0.2592	0.2593	0.2593	0.2594	0.2594	0.2495	-0.6346	-1.1398
12 WSS	-2.5138	-0.8700	0.4165	0.4300	0.4299	0.4301	0.4299	0.4298	0.4298	0.4299	0.4301	0.4299	0.4300	0.4165	-0.8700	-2.5138
14 WSS	-15.4192	0.2886	0.6077	0.6089	0.6089	0.6086	0.6089	0.6087	0.6087	0.6089	0.6086	0.6089	0.6089	0.6077	0.2886	-15.4192
16 WSS	-16.7938	0.2420	0.6197	0.6207	0.6208	0.6208	0.6210	0.6210	0.6210	0.6210	0.6208	0.6208	0.6207	0.6197	0.2420	-16.7938
18 WSS	-18.1189	0.1913	0.6307	0.6320	0.6320	0.6320	0.6320	0.6321	0.6321	0.6320	0.6320	0.6320	0.6320	0.6307	0.1913	-18.1189
20 WSS	-19.4097	0.1376	0.6411	0.6425	0.6427	0.6426	0.6423	0.6427	0.6427	0.6423	0.6426	0.6427	0.6425	0.6411	0.1376	-19.4097

Table 3.7: Power Ratios per subcarrier using Power Loading strategy with $\alpha = \alpha_{opt}$ and SNR[dB] = required SNR at α_{opt} for $N_{WSS} \in \{0,..,20\}$, HD-FEC

3.4.4 Bit&Power Loading

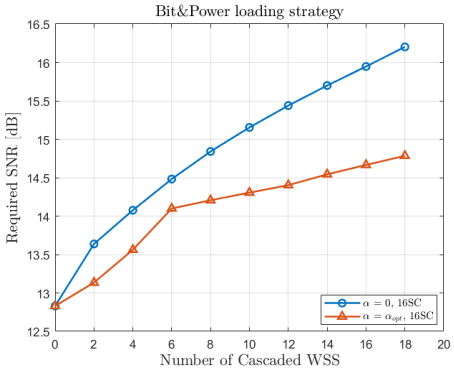

Figure 3.31: Required SNR [dB] vs. N_{WSS} with $\alpha = 0$ and $\alpha = \alpha_{opt}$ for $N_{WSS} \in \{0,..,20\}$, 16SCs SD-FEC , Bit&Power Loading strategy

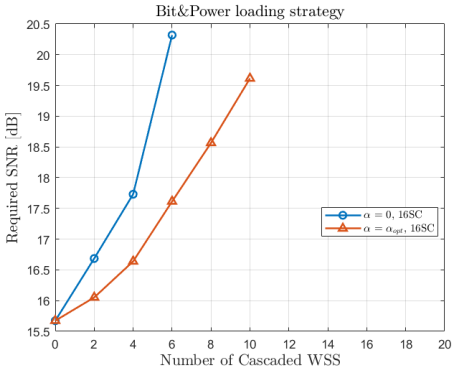

Figure 3.32: Required SNR [dB] vs. N_{WSS} with $\alpha = 0$ and $\alpha = \alpha_{opt}$ for $N_{WSS} \in \{0,..,20\}$, 16SCs HD-FEC , Bit&Power Loading strategy

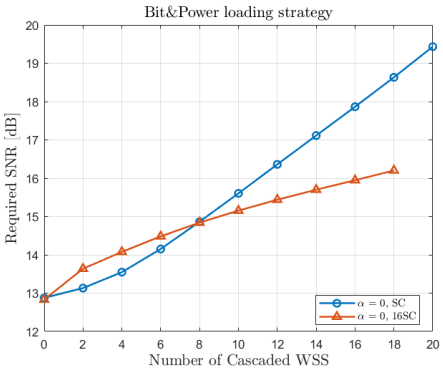

Figure 3.33: Required SNR [dB] vs. N_{WSS} with $\alpha = 0$ SC and $\alpha = 0$ 16SCs for $N_{WSS} \in \{0,..,20\}$, SD-FEC, Bit&Power Loading strategy

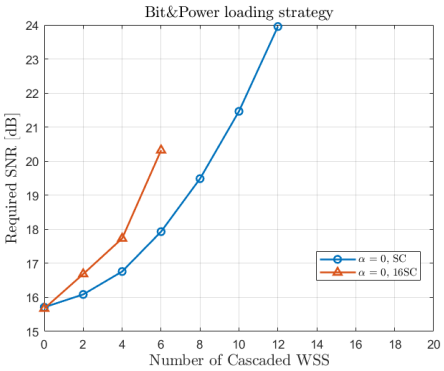

Figure 3.34: Required SNR [dB] vs. N_{WSS} with $\alpha = 0$ SC and $\alpha = 0$ 16SCs for $N_{WSS} \in \{0,..,20\}$, HD-FEC, Bit&Power Loading strategy

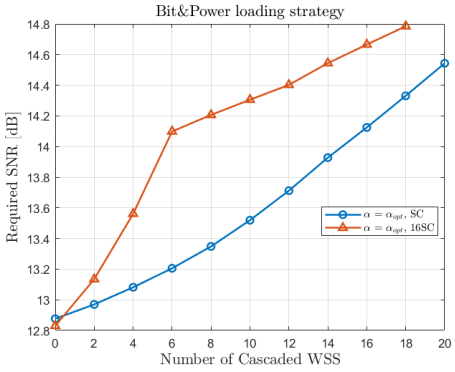

Figure 3.35: Required SNR [dB] vs. N_{WSS} with $\alpha = \alpha_{opt}$ SC and $\alpha = \alpha_{opt}$ 16SCs for $N_{WSS} \in \{0,..,20\}$, SD-FEC, Bit&Power Loading strategy

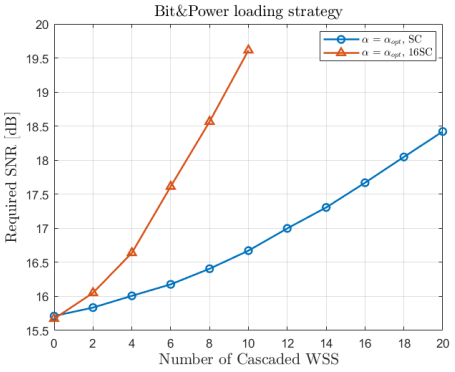

Figure 3.36: Required SNR [dB] vs. N_{WSS} with $\alpha = \alpha_{opt}$ SC and $\alpha = \alpha_{opt}$ 16SCs for $N_{WSS} \in \{0,..,20\}$, HD-FEC, Bit&Power Loading strategy

In this scenario, the Bit&Power Loading strategy was applied, actually combining the benefits of both BL and PL strategies. The observed trends, generally, closely resemble to those of the other techniques analyzed up to now. However, it is possible to notice from Fig. 3.33, the application of BPL in the SD-FEC case with $\alpha = 0$ clearly outperforms the single-carrier scenario when a N_{WSS} behind 8 is analyzed. This observation underscores the effectiveness of the SCM method to enhance system capabilities and achieving better performance outcomes.

3.4.5 Water Filling

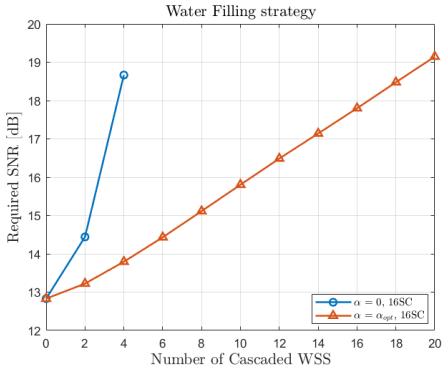

Figure 3.37: Required SNR [dB] vs. N_{WSS} with $\alpha = 0$ and $\alpha = \alpha_{opt}$ for $N_{WSS} \in \{0,..,20\}$, 16SCs SD-FEC , Water Filling strategy

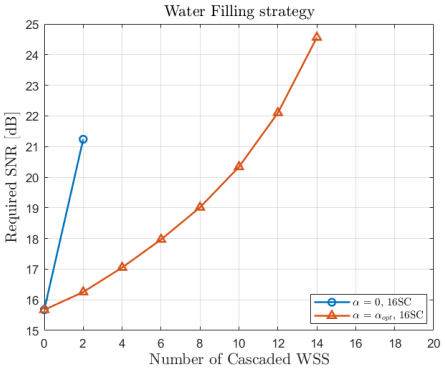

Figure 3.38: Required SNR [dB] vs. N_{WSS} with $\alpha = 0$ and $\alpha = \alpha_{opt}$ for $N_{WSS} \in \{0,..,20\}$, 16SCs HD-FEC , Water Filling strategy

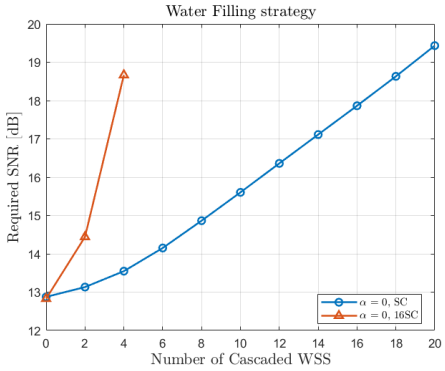

Figure 3.39: Required SNR [dB] vs. N_{WSS} with $\alpha = 0$ SC and $\alpha = 0$ 16SCs for $N_{WSS} \in \{0,..,20\}$, SD-FEC, Water Filling strategy

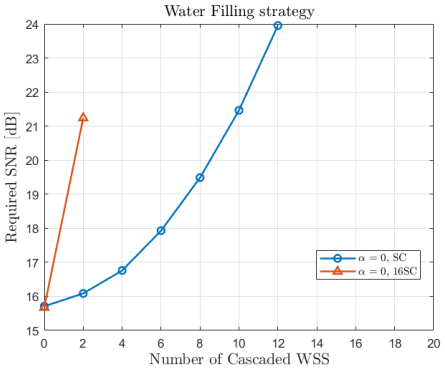

Figure 3.40: Required SNR [dB] vs. N_{WSS} with $\alpha = 0$ SC and $\alpha = 0$ 16SCs for $N_{WSS} \in \{0,..,20\}$, HD-FEC, Water Filling strategy

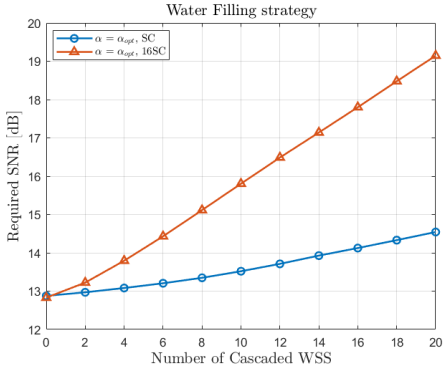

Figure 3.41: Required SNR [dB] vs. N_{WSS} with $\alpha = \alpha_{opt}$ SC and $\alpha = \alpha_{opt}$ 16SCs for $N_{WSS} \in \{0,..,20\}$, SD-FEC, Water Filling strategy

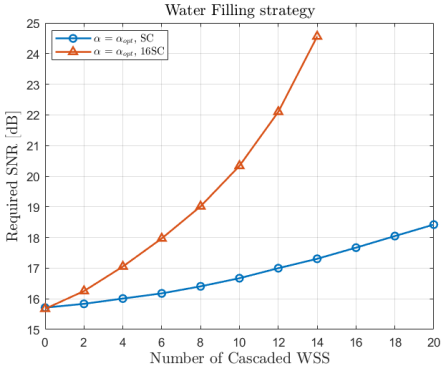

Figure 3.42: Required SNR [dB] vs. N_{WSS} with $\alpha = \alpha_{opt}$ SC and $\alpha = \alpha_{opt}$ 16SCs for $N_{WSS} \in \{0,..,20\}$, HD-FEC, Water Filling strategy

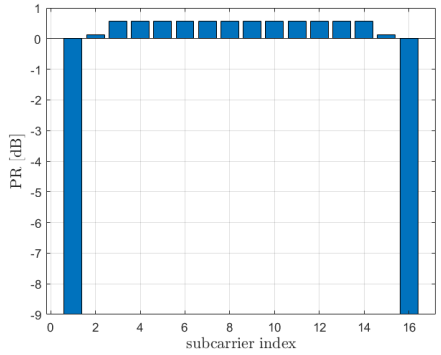

Figure 3.43: Pictorial representation of Power Ratios per subcarrier using Water Filling strategy with $\alpha = 0$, SNR[dB] = 25, $N_{WSS} = 10$, SD-FEC

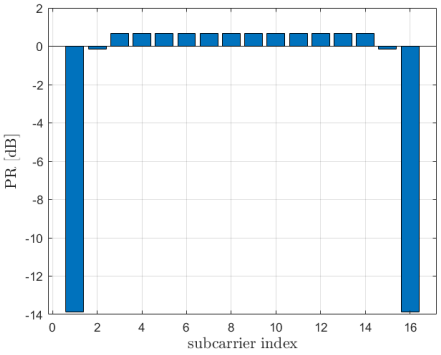

Figure 3.44: Pictorial representation of Power Ratios per subcarrier using Water Filling strategy with $\alpha = 0$, SNR[dB] = 25, $N_{WSS} = 20$, SD-FEC

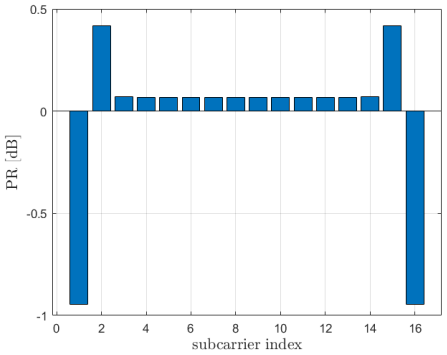

Figure 3.45: Pictorial representation of Power Ratios per subcarrier using Water Filling strategy with $\alpha = 0.26$, SNR[dB] = 25, $N_{WSS} = 10$, SD-FEC

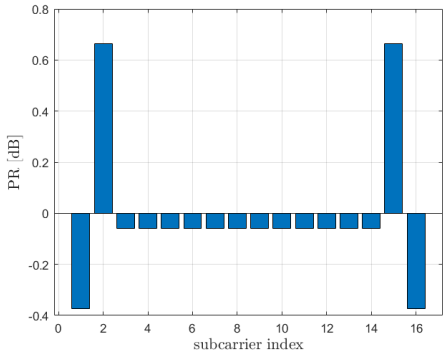

Figure 3.46: Pictorial representation of Power Ratios per subcarrier using Water Filling strategy with $\alpha = 0.26$, SNR[dB] = 25, $N_{WSS} = 20$, SD-FEC

The final optimization strategy analyzed is the Water-Filling technique. As defined in Sect.2.2, this method dynamically allocates power across subcarriers based on their respective experienced SNR. Observing the results shown in Figg. 3.43-3.44, it is evident that the power allocated to the outer subcarriers, which are more affected from the cascaded filtering effects, is minimal, reflecting their relatively poor SNR values. However, when an average optimal value of $\alpha = 0.26$ is employed, as shown in Figg. 3.45-3.46, significant differences become apparent. Specifically, the enhancement introduced on the transfer function's shape by this adjustment, mitigates the filtering penalties previously experienced by the outer subcarriers as the number of cascaded filter increases. Consequently, their allocated power levels become higher compared to the case with $\alpha = 0$, enabling a more equitable power distribution.

3.4.6 Final comparison Uniform QAM case

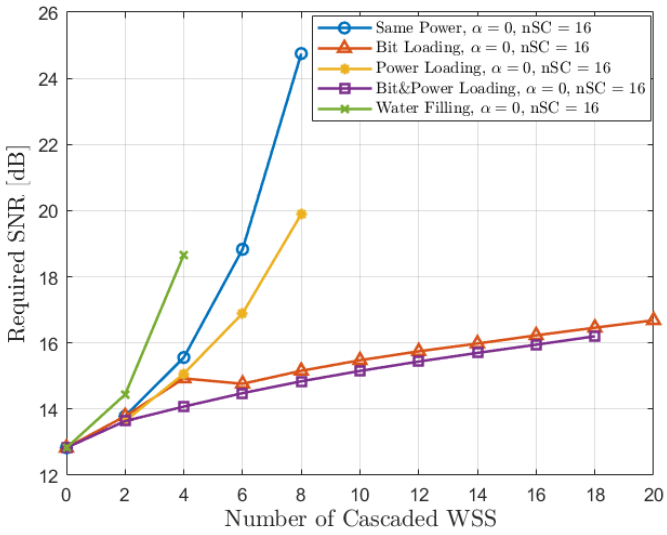

Figure 3.47: Comparison between all the optimization strategies, Required SNR [dB] vs. N_{WSS} with $\alpha = 0$ for $N_{WSS} \in \{0,..,20\}$, 16SCs SD-FEC

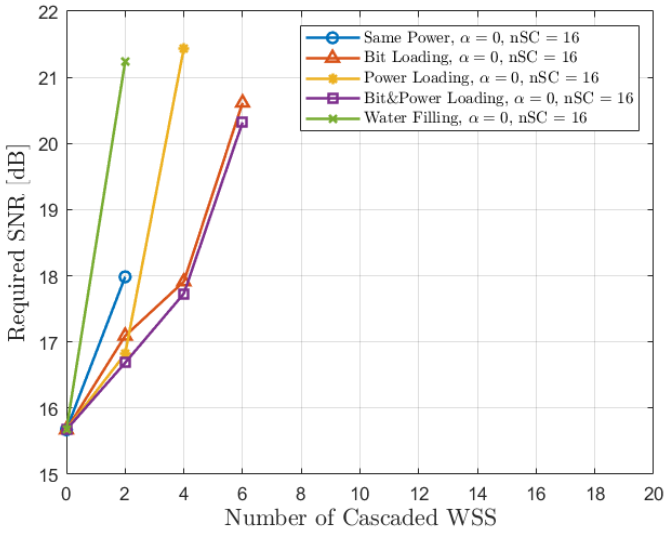

Figure 3.48: Comparison between all the optimization strategies, Required SNR [dB] vs. N_{WSS} with $\alpha = 0$ for $N_{WSS} \in \{0,..,20\}$, 16SCs HD-FEC

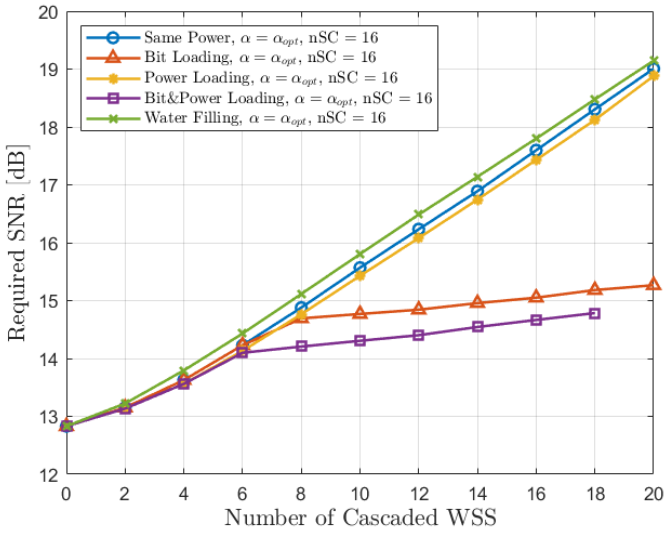

Figure 3.49: Comparison between all the optimization strategies, Required SNR [dB] vs. N_{WSS} with $\alpha = \alpha_{opt}$for $N_{WSS} \in \{0,..,20\}$, 16SCs SD-FEC

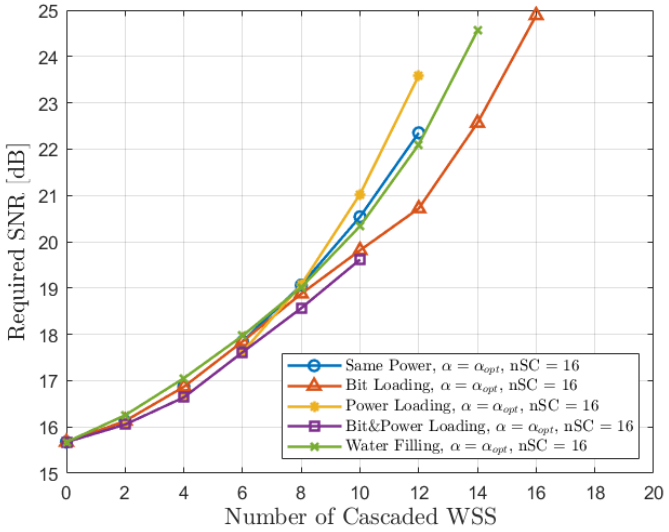

Figure 3.50: Comparison between all the optimization strategies, Required SNR [dB] vs. N_{WSS} with $\alpha = \alpha_{opt}$for $N_{WSS} \in \{0,..,20\}$, 16SCs HD-FEC

After evaluating all the optimization strategies, both with and without Bandwidth Enhancement, the following insights emerged. As observed from the result plots presented

in this section (Figg.3.47-3.50), the trend of the minimum SNR required as the number of cascaded WSS increases, remains generally the same across all the 4 scenarios introduced (i.e. α =0 and $\alpha = \alpha_{opt}$ for both HD-FEC and SD-FEC). However, it is noteworthy from Fig. 3.50 that in the HD-FEC case with BE, when the number of WSS exceeds 8, the Power Loading strategy applied to 16 subcarriers becomes the least effective, performing worse than both the Water Filling and the Same Power strategies, which were identified as the least effective in other cases. Furthermore, it can be clearly seen that, the introduction of BE enabled the optimization of the parameter α, allowing these strategies to remain effective even when a large number of cascaded WSS are considered. Comparing Fig. 3.48 and Fig. 3.50 highlights this improvement: without BE (Fig. 3.48), the SNR required to implement these techniques becomes impractically high as the number of WSS increases. In contrast, with BE and by considering an α near to its optimum value, the required SNR values are significantly reduced, enabling the application of these techniques with up to 16 cascaded WSS while requiring a maximum SNR of 25 dB which is a feasible value within the current optical communication systems.

3.5 PCS comparison

This section will be dedicated to shown the outcomes obtained using PCS. The simulation scenario remained almost equal with respect to the one employed for Uniform QAM. However, some adjustments were introduced to adapt to PCS. The primary change was the adoption of GMI as the evaluation metric instead of the BER with a target GMI value set to 3.33. This adaptation allows for a more detailed analysis of the PCS. In addition, multiple starting modulation formats were considered (M_{PCS}), specifically 64-QAM, 256-QAM. However, due to prohibitive computational costs, the analysis for 256-QAM was limited to the scenario without BE, thus, $\alpha = 0$.

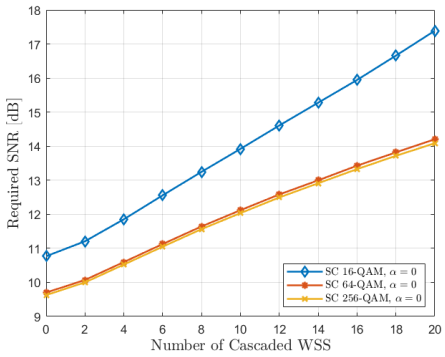

Figure 3.51: Required SNR [dB] vs. N_{WSS} with $\alpha = 0$ for $N_{WSS} \in \{0,..,20\}$ using PCS with starting constellations 64-QAM/256-QAM and Uniform 16-QAM, SC SD-FEC

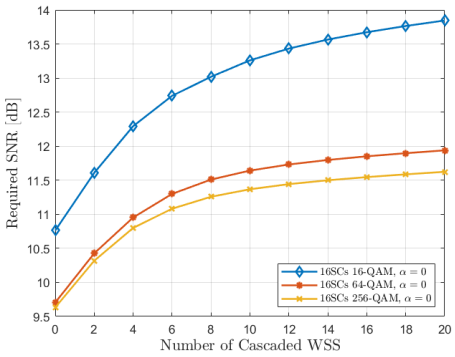

Figure 3.52: Required SNR [dB] vs. N_{WSS} with $\alpha = 0$ for $N_{WSS} \in \{0,..,20\}$ using PCS with starting constellations 64-QAM/256-QAM and Uniform 16-QAM, 16SCs SD-FEC

From Fig. 3.51 and Fig. 3.52, it is evident that the use of PCS significantly improves performance, requiring a lower SNR to achieve the target GMI compared to when a uniform QAM constellation is used. This improvement is particularly pronounced in MSC systems.

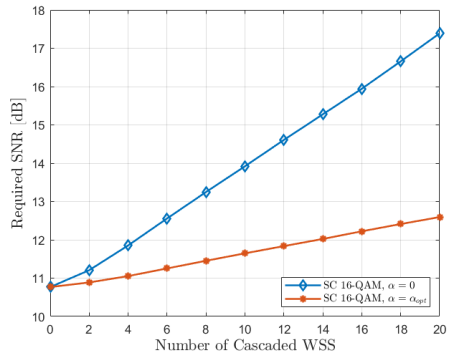

Figure 3.53: Required SNR [dB] vs. N_{WSS} with $\alpha = 0$ and $\alpha = \alpha_{opt}$ for $N_{WSS} \in \{0,..,20\}$ using Uniform 16-QAM, 16SCs constellation, SC SD-FEC

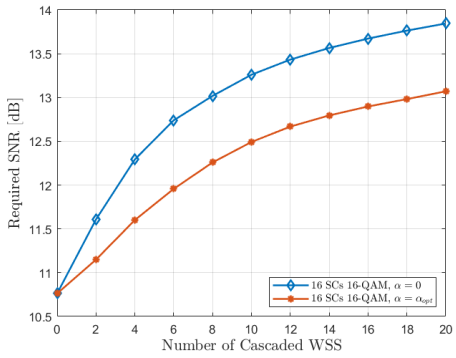

Figure 3.54: Required SNR [dB] vs. N_{WSS} with $\alpha = 0$ and $\alpha = \alpha_{opt}$ for $N_{WSS} \in \{0,..,20\}$ using Uniform 16-QAM, 16SCs constellation, SD-FEC

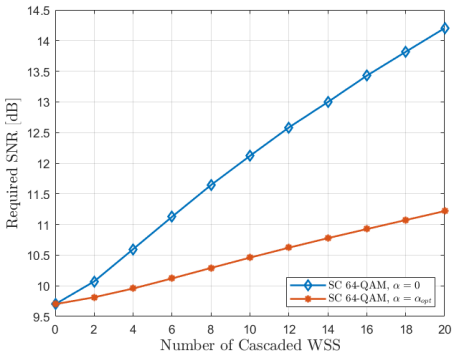

Figure 3.55: Required SNR [dB] vs. N_{WSS} with $\alpha = 0$ and $\alpha = \alpha_{opt}$ for $N_{WSS} \in \{0,..,20\}$ using PCS with starting constellation 64-QAM, SC SD-FEC

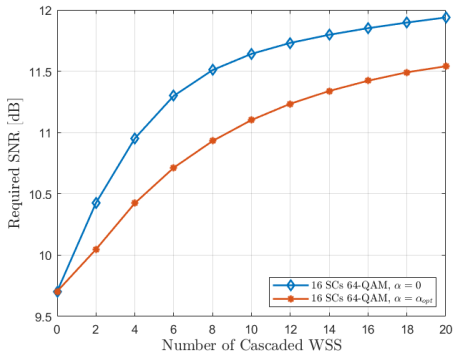

Figure 3.56: Required SNR [dB] vs. N_{WSS} with $\alpha = 0$ and $\alpha = \alpha_{opt}$ for $N_{WSS} \in \{0,..,20\}$ using PCS with starting constellation 64-QAM, 16SCs SD-FEC

Furthermore, the introduction of BE combined with PCS provides additional benefits, as shown in Fig. 3.55 and Fig. 3.56. Notably, in the SC case (Fig. 3.55), a gain of approximately 3 dB in terms of required SNR is achieved when 20 cascaded WSS are considered. Conversely, this gain is less substantial in MSC systems, as observed in Fig. **??**, where it amounts to approximately 0.5 dB in the case of 20 cascaded WSS.

Chapter 4

Conclusions

This thesis aims at evaluating the results of BE's integration in the WSS in optical communication networks as an effective candidate to counteract the narrowing filtering effects. This approach has been also coupled with the use of different optimization strategies to reach the main goal. In this work, the presented transmission system is a 800 Gbit/s with different symbol rate according to the FEC type used. A total symbol rate of 128 Gbaud has been considered in SD-FEC systems and of 112 Gbaud if the system was an HD-FEC one. The analyzed modulation techniques are divided into two main groups, Uniform QAM constellation and Probabilistic Shaped Constellation. Furthermore, the different optimization strategies proposed rely on the use of subcarrier multiplexing and advanced bit and/or power loading techniques to reduce filtering effects caused by the increasing number of WSS, in this thesis up to 20 with a step size equal to 2. To find the best solution, the minimum SNR to reach the BER/GMI target has been evalutated and compared across all the different optimization strategies, considering them both jointly or not with the BE. In addition, it has emerged that among all the possible optimization strategies used in Uniform QAM constellation, the one that performs better is the Bit&Power loading, which turns out to be an acceptable compromise between benefits and computational costs. The research also highlights the ability of WSS with BE to strike a balance between robustness and spectral efficiency. This balance is crucial for operating in noise-prone environments while maintaining high efficiency in dense optical channels. The flexibility and versatility of WSS technology are pivotal in meeting the increasing demands of modern optical networks, which are constantly evolving to handle larger volumes of data. Indeed , the anticipated launch of the Sixth Generation (6G) of mobile technology by 2030 will mark a significant milestone in the evolution of wireless communication, delivering unprecedented advancements in technology and applications. 6G is expected to deliver ultra-high data rates and almost instantaneous communications, with three-dimensional coverage for everything, everywhere, and at any time. Optical technologies are expected to play a vital role in realizing the 6G fronthaul infrastructure, offering the high-speed, low-latency, and reliable transmission needed to meet the stringent demands of 6G networks [31]. This work could be further extended, analyzing different modulation format to be used in Uniform QAM case and considering

different number of subcarriers, substituting the PM-16QAM and the 16 subcarriers used up to now.

Bibliography

[1] Shiva Kumar and M Jamal Deen. *Fiber optic communications: fundamentals and applications*. John Wiley & Sons, 2014.

[2] David A. Simpson. "Spectroscopy of thulium doped silica glass". In: *Spectroscopy of thulium doped silica glass*. 2008.

[3] R. Paschotta. *Cladding Modes*. RP Photonics Encyclopedia. URL: https://www.rp-photonics.com/cladding_modes.html.

[4] Wayne S. Pelouch. "Raman Amplification: An Enabling Technology for Long-Haul Coherent Transmission Systems". In: *Journal of Lightwave Technology* 34.1 (2016), pp. 6–19. DOI: 10.1109/JLT.2015.2458771.

[5] Darli Augusto de Arruda Mello and Fabio Aparecido Barbosa. *Digital Coherent Optical Systems*. Springer, 2021.

[6] Md. Saifuddin Faruk and Seb J. Savory. "Digital Signal Processing for Coherent Transceivers Employing Multilevel Formats". In: *Journal of Lightwave Technology* 35.5 (2017), pp. 1125–1141. DOI: 10.1109/JLT.2017.2662319.

[7] Léia de Sousa and André Drummond. *Metropolitan Optical Networks: A Survey on New Architectures and Future Trends*. Jan. 2022. DOI: 10.48550/arXiv.2201.10709.

[8] S. Voloshynovskiy et al. "Information-Theoretic Data-Hiding: Recent Achievements And Open Problems." In: *Int. J. Image Graphics* 5 (Jan. 2005), pp. 5–36.

[9] Timo Pfau, Sebastian Hoffmann, and Reinhold Noe. "Hardware-Efficient Coherent Digital Receiver Concept With Feedforward Carrier Recovery for M -QAM Constellations". In: *Journal of Lightwave Technology* 27.8 (2009), pp. 989–999.

[10] Andrea Carena Roberto Gaudino. "Course of "Optical and Wireless Communications"". Politecnico di Torino. 2021/2022.

[11] Mehdi Torbatian et al. "Performance Oriented DSP for Flexible Long Haul Coherent Transmission". In: *Journal of Lightwave Technology* 40.5 (2022), pp. 1256–1272.

[12] Giuseppe Rizzelli, Pablo Torres-Ferrera, and Roberto Gaudino. "An Analytical Model for Coherent Transmission Performance Estimation After Generic Jones Matrices". In: *Journal of Lightwave Technology* 41.14 (2023), pp. 4582–4589.

[13] Meng Qiu et al. "Subcarrier multiplexing using DACs for fiber nonlinearity mitigation in coherent optical communication systems". In: *OFC 2014*. 2014, pp. 1–3.

[14] Han Sun et al. "800G DSP ASIC Design Using Probabilistic Shaping and Digital Sub-Carrier Multiplexing". In: *Journal of Lightwave Technology* 38.17 (2020), pp. 4744–4756. DOI: 10.1109/JLT.2020.2996188.

[15] A. Devarajan et al. "Colorless, Directionless and Contentionless multi-degree ROADM architecture for mesh optical networks". In: *COMSNETS 2010*. Feb. 2010, pp. 1–10.

[16] Yiran Ma et al. "Recent Progress of Wavelength Selective Switch". In: *Journal of Lightwave Technology* 39.4 (2021), pp. 896–903.

[17] Cibby Pulikkaseril et al. "Spectral modeling of channel band shapes in wavelength selective switches". In: *Optics express* 19 (Apr. 2011), pp. 8458–70.

[18] Takashi Inoue, Ryosuke Matsumoto, and Kiyo Ishii. "Quality Analysis of Uniform and PS QAM Signals Distorted by Arbitrary Filtering Effects of WSS in ROADM-Based Optical Network". In: *Journal of Lightwave Technology* 42.15 (2024), pp. 5099–5112.

[19] Talha Rahman et al. "On the Mitigation of Optical Filtering Penalties Originating From ROADM Cascade". In: *IEEE Photonics Technology Letters* 26.2 (2014), pp. 154–157.

[20] Mohsin Fayyaz, Khurram Aziz, and Ghulam Mujtaba. "Performance analysis of optical interconnects' architectures for data center networks: Do you have a subtitle? If so, write it here". In: *Cluster Computing* 19 (Sept. 2016).

[21] Fernando Pedro Guiomar et al. "Frequency-Domain Hybrid Modulation Formats for High Bit-Rate Flexibility and Nonlinear Robustness". In: *Journal of Lightwave Technology* 36.20 (2018), pp. 4856–4870. DOI: 10.1109/JLT.2018.2866625.

[22] Trung-Hien Nguyen et al. "Quantifying the Gain of Entropy-Loaded Digital Multicarrier for Beyond 100 Gbaud Transmission Systems". In: *2021 Optical Fiber Communications Conference and Exhibition (OFC)*. 2021, pp. 1–3.

[23] Ann Rosa Brusin et al. "Enhanced resilience towards ROADM-induced optical filtering using subcarrier multiplexing and optimized bit and power loading". In: *Optics Express* 27 (Oct. 2019), p. 30710. DOI: 10.1364/OE.27.030710.

[24] Junho Cho and Peter J. Winzer. "Probabilistic Constellation Shaping for Optical Fiber Communications". In: *Journal of Lightwave Technology* 37.6 (2019), pp. 1590–1607.

[25] Fernando P. Guiomar et al. "Adaptive Probabilistic Shaped Modulation for High-Capacity Free-Space Optical Links". In: *Journal of Lightwave Technology* 38.23 (2020), pp. 6529–6541. DOI: 10.1109/JLT.2020.3012737.

[26] Si-Ao Li et al. "Enabling Technology in High-Baud-Rate Coherent Optical Communication Systems". In: *IEEE Access* 8 (2020), pp. 111318–111329.

[27] Di Che and William Shieh. "Squeezing out the last few bits from band-limited channels with entropy loading". In: *Opt. Express* 27.7 (Apr. 2019), pp. 9321–9329. URL: https://opg.optica.org/oe/abstract.cfm?URI=oe-27-7-9321.

[28] Qiaoya Liu et al. "Subcarrier-pairing entropy loading for digital subcarrier-multiplexing systems with colored-SNR distributions". In: *Opt. Express* 29.18 (Aug. 2021), pp. 28852–28863. DOI: 10.1364/OE.434742. URL: https://opg.optica.org/oe/abstract.cfm?URI=oe-29-18-28852.

[29] Di Che and William Shieh. "Approaching the Capacity of Colored-SNR Optical Channels by Multicarrier Entropy Loading". In: *Journal of Lightwave Technology* 36.1 (2018), pp. 68–78. DOI: 10.1109/JLT.2017.2778290.

[30] Patrick Blown et al. "Optical Bandwidth Enhancement Modelling for Cascaded WSS". In: *2022 Asia Communications and Photonics Conference (ACP)*. 2022, pp. 1303–1305. DOI: 10.1109/ACP55869.2022.10088732.

[31] Abdulhalim Fayad, Tibor Cinkler, and Jacek Rak. "Toward 6G Optical Fronthaul: A Survey on Enabling Technologies and Research Perspectives". In: *IEEE Communications Surveys & Tutorials* (2024), pp. 1–1. DOI: 10.1109/COMST.2024.3408090.